

Article

Chemical Modification of Dental Dimethacrylate Copolymer with Tetramethylxylene Diisocyanate-Based Quaternary Ammonium Urethane-Dimethacrylates—Physicochemical, Mechanical, and Antibacterial Properties

Patryk Drejka ¹, Marta Chrószcz-Porębska ¹, Alicja Kazek-Kęsik ^{2,3}, Grzegorz Chladek ⁴
and Izabela Barszczewska-Rybarek ^{1,*}

¹ Department of Physical Chemistry and Technology of Polymers, Faculty of Chemistry, Silesian University of Technology, Strzody 9 Str., 44-100 Gliwice, Poland; patryk.drejka@polsl.pl (P.D.); marta.chroszcz.porebska@gmail.com (M.C.-P.)

² Department of Inorganic Chemistry, Analytical Chemistry and Electrochemistry, Faculty of Chemistry, Silesian University of Technology, Krzywoustego 6 Str., 44-100 Gliwice, Poland; alicja.kazek-kesik@polsl.pl

³ Biotechnology Centre, Silesian University of Technology, Krzywoustego 8 Str., 44-100 Gliwice, Poland

⁴ Department of Engineering Materials and Biomaterials, Faculty of Mechanical Engineering, Silesian University of Technology, Konarskiego 18A Str., 44-100 Gliwice, Poland; grzegorz.chladek@polsl.pl

* Correspondence: izabela.barszczewska-rybarek@polsl.pl; Tel.: +48-32-237-1793

Abstract: In this study, two novel quaternary ammonium urethane-dimethacrylates (QAUDMAs) were designed for potential use as comonomers in antibacterial dental composite restorative materials. QAUDMAs were synthesized via the reaction of 1,3-bis(1-isocyanato-1-methylethyl)benzene with 2-(methacryloyloxy)ethyl-2-decylhydroxyethylmethylammonium bromide (QA10+TMXDI) and 2-(methacryloyloxy)ethyl-2-dodecylhydroxyethylmethylammonium bromide (QA12+TMXDI). Their compositions with common dental dimethacrylates comprising QAUDMA 20 wt.%, urethane-dimethacrylate monomer (UDMA) 20 wt.%, bisphenol A glycerolate dimethacrylate (Bis-GMA) 40 wt.%, and triethylene glycol dimethacrylate (TEGDMA) 20 wt.%, were photocured. The achieved copolymers were characterized for their physicochemical and mechanical properties, including their degree of conversion (*DC*), glass transition temperature (*T_g*), polymerization shrinkage (*S*), water contact angle (*WCA*), flexural modulus (*E*), flexural strength (*FS*), hardness (*HB*), water sorption (*WS*), and water leachability (*WL*). The antibacterial activity of the copolymers was characterized by the minimum bactericidal concentration (*MBC*) and minimum inhibitory concentration (*MIC*) against *Staphylococcus aureus* and *Escherichia coli*. The achieved results were compared to the properties of a typical dental copolymer comprising UDMA 40 wt.%, Bis-GMA 40 wt.%, and TEGDMA 20 wt.%. The introduction of QAUDMAs did not deteriorate physicochemical and mechanical properties. The *WS* and *WL* increased; however, they were still satisfactory. The copolymer comprising QA10+TMXDI showed a higher antibacterial effect than that comprising QA12+TMXDI and that of the reference copolymer.

Keywords: dental resin; urethane-dimethacrylate; quaternary ammonium; copolymerization; photocuring; antibacterial properties; physicochemical properties; mechanical properties



Citation: Drejka, P.;

Chrószcz-Porębska, M.; Kazek-Kęsik, A.; Chladek, G.; Barszczewska-Rybarek, I. Chemical Modification of Dental Dimethacrylate Copolymer with Tetramethylxylene Diisocyanate-Based Quaternary Ammonium Urethane-Dimethacrylates—Physicochemical, Mechanical, and Antibacterial Properties. *Materials* **2024**, *17*, 298. <https://doi.org/10.3390/ma17020298>

Academic Editor: Abderrahim Yassar

Received: 18 December 2023

Revised: 1 January 2024

Accepted: 5 January 2024

Published: 7 January 2024



Copyright: © 2024 by the authors. Licensee MDPI, Basel, Switzerland. This article is an open access article distributed under the terms and conditions of the Creative Commons Attribution (CC BY) license (<https://creativecommons.org/licenses/by/4.0/>).

1. Introduction

Faced with the increase in the dental caries scale [1,2], it is important to find effective solutions for curing this disease. Therefore, in recent years, an upward trend in the development of antimicrobial dental composite restorative materials (DCRMs) is observed [3–15]. The elementary concept of providing DCRMs with antimicrobial properties assumes physically dispersing bioactive substances (such as antibiotics, antimicrobial enzymes, chlorhexidine, triclosan, metals, metal oxides, and the nanoparticles of quaternized

polyethyleneimine) in available dental materials [5–12,14]. As these types of biocides can easily elute from a material, the material achieved shows only a short-term antimicrobial effect. It quickly loses its mechanical and antimicrobial properties and causes cytotoxic effects [16,17].

Another concept of providing DCRMs with antimicrobial properties is based on the covalent incorporation of a monomeric biocide into the polymer network structure, constituting the DCRM matrix. It involves the copolymerization of universal dental dimethacrylates (DMAs), such as bisphenol A glycerolate dimethacrylate (Bis-GMA), its ethoxylated derivative (Bis-EMA), urethane-dimethacrylate monomer (UDMA), and triethylene glycol dimethacrylate (TEGDMA), with dimethacrylates having bioactive groups, of which dimethacrylates with quaternary ammonium (QA) groups (QADMA) are the best known [18–22]. The QADMA content in a copolymer ranges from a few to several dozen percent. This alternative offers the stable, non-leaching, and long-term antimicrobial action of a DCRM [23,24]. The huge advantages of monomeric antimicrobials include lower cytotoxic effects in comparison to physically dispersed antibacterial agents [16,25] and an alternative to antibiotics, whose application should be limited due to the increasing resistance of microorganisms [26–28]. The aforementioned features of QADMA explain the great interest among scientists in designing novel monomer structures containing QA groups and the development of related materials.

The following series of QADMA are described in the literature:

- (i) dimethacrylate derivatives of *N*-methyl-diethanolamine (MDEA) with one central quaternary ammonium group (QAn+MDEA, where *n* is the number of carbon atoms in the *N*-alkyl substituent of the QA group). QA12+MDEA and QA16+MDEA were studied [29,30];
- (ii) dimethacrylate derivatives of *N,N*-dimethylaminoethyl methacrylate (DMAEMA) with two QA groups separated with a central aliphatic chain (QAn+DMAEMA, where *n* is the number of carbon atoms in the chain separating QA groups). QA groups in these monomers were substituted with two methyl groups. QA4+DMAEMA and QA6+DMAEMA were studied [31];
- (iii) the Bis-GMA quaternary ammonium derivative with two QA groups (QAn+bis-GMA, where *n* is the number of carbon atoms in the *N*-alkyl substituent of the QA group). QA6+bis-GMA was studied [32];
- (iv) fully aliphatic urethane-dimethacrylates with one central QA group, based on *N*-methyl-diethanolamine (MDEA) and 2-isocyanatoethyl methacrylate (IEM) (QAn+MDEA+IEM, where *n* is the number of carbon atoms in the *N*-alkyl substituents of the QA group). QAn+MDEA+IEMs with *n* of 12, 14, 16, and 18 were studied [33,34];
- (v) urethane-dimethacrylates with one central QA group, based on *N*-methyl-diethanolamine (MDEA) and cycloaliphatic isophorone diisocyanate (IPDI) (QAn+MDEA+IPDI, where *n* is the number of carbon atoms in the *N*-alkyl substituent of the QA group). QAn+MDEA+IPDI with *n* of 12, 14, 16, and 18 were studied [35,36];
- (vi) quaternary ammonium analogues of the urethane-dimethacrylate monomer with two QA groups (QAn+TMDI, where *n* is the number of carbon atoms in the *N*-alkyl substituent of the QA group). QAn+TMDI with *n* of 8, 10, 12, 14, 16, and 18 were studied [37–42].

QAn+MDEAs showed high antibacterial activity against many bacteria strains, including *S. aureus*, *Streptococcus mutans*, *Actinomyces viscosus*, *Lactobacillus acidophilus*, *Streptococcus sanguinis*, *Porphyromonas gingivalis*, *Prevotella melaninogenica*, and *Enterococcus faecalis*. In addition, these monomers showed cytotoxicity lower than Bis-GMA [29]. The copolymer of QAn+MDEA 10 wt.% with Bis-GMA/TEGDMA 90 wt.% showed antibacterial activity against *S. mutans* [30]. QAn+DMAEMA 1 wt.% was used to modify a commercial adhesive resin (Tetric N-Bond) and the resulting material also showed antibacterial activity against *S. mutans* [31]. The introduction of QAn+Bis-GMA 5 wt.% into the Bis-GMA/TEGDMA formulation resulted in a copolymer with antibacterial activity against *E. coli*, *S. aureus*, *S. mutans*, and *Bacillus subtilis*. The antifungal activity of the modified copolymer against

Candida albicans was observed too. As the QAn+Bis-GMA concentration increased, the antimicrobial activity increased; however, it was accompanied by an increase in cytotoxicity and the deterioration of mechanical properties [32]. The modification of the same Bis-GMA/TEGDMA formulation with QAn+MDEA+IEM 5 wt.% resulted in an antibacterial copolymer only for QA16+MDEA+IEM. It showed antibacterial activity against *S. mutans*. All other copolymers gained antibacterial activity as the QAn+MDEA+IEMs concentration increased to 10 wt.%, but this was accompanied by the deterioration in mechanical properties [33,34]. The QAn+MDEA+IPDI 50 wt.% and TEGDMA 50 wt.% copolymers also showed high antibacterial activity against *S. mutans*. However, the disadvantages of these copolymers included a low flexural strength, low modulus of elasticity, and high water sorption [35,36]. By reducing the QAn+MDEA+IPDI content to 30 wt.% and using a formulation of Bis-GMA/TEGDMA 70 wt.%, an improvement in mechanical properties was achieved [36]. QAn+TMDIs and their copolymers were the most extensively studied [37–42]. Copolymers of QAn+TMDI 60 wt.% and TEGDMA 40 wt.% were characterized by very high antibacterial activity against *S. aureus* and *E. coli*. However, they had insufficiently good mechanical parameters, excessively high water sorption, and water leachability [38,39]. Copolymers of QAn+TMDI 40 wt.%, Bis-GMA 40 wt.%, and TEGDMA 20 wt.% also showed high antimicrobial activity against *S. aureus* and *E. coli* [40]. In addition, antifungal activity against *C. albicans* was observed for these copolymers [41]. Many of their physicochemical, mechanical, and biological parameters were good. However, the detailed analysis showed that an increase in the *N*-alkyl substituent length resulted in a decrease in the antibacterial activity, and the deterioration of mechanical properties [40–42]. This analysis led to the conclusion that copolymers based on QA10+TMDI and QA12+TMDI contain the optimum combination of properties [40].

The promising results obtained for copolymers based on QA10+TMDI and QA12+TMDI motivated us to replace the TMDI core with a 1,3-bis(1-isocyanate-1-methylethyl)benzene (TMXDI) core to obtain new urethane-dimethacrylate monomers with two QA groups located in the wings and 1,3-phenylene ring located in the core. We formulated a hypothesis that the copolymerization of the achieved quaternary ammonium urethane-dimethacrylates (QAUDMAs) with UDMA, Bis-GMA, and TEGDMA results in an antibacterial copolymer with good physicochemical and mechanical properties. Therefore, the goal of this work was to synthesize two novel urethane-dimethacrylates with the TMXDI core and two methacrylate-ended wings comprising the QA group in the middle. The QA groups were substituted with an *N*-alkyl chain of 10 and 12 carbon atoms (QA10+TMXDI and QA12+TMXDI, respectively). The two novel monomers were compounded with common dental dimethacrylates in the following weight fractions: QAUDMA 20 wt.%, UDMA 20 wt.%, Bis-GMA 40 wt.%, and TEGDMA 20 wt.%. The two novel monomers were also photocured. The novel monomers, as well as their compositions with dental dimethacrylates, were characterized for molecular weight (*MW*), concentration of double bonds (x_{DB}), viscosity (η), refractive index (*RI*), and density (d_m). The degree of conversion (*DC*), density (d_p), polymerization shrinkage (*S*), glass transition temperature (T_g), water contact angle (*WCA*), water sorption (*WS*), water solubility (*SL*), hardness (*HB*), flexural strength (*FS*), flexural modulus (*E*), minimum bactericidal concentration (*MBC*), and minimum inhibitory concentration (*MIC*) were all measured for the resulting copolymers (the first comprising QA10+TMXDI (20(QA10+TMXDI)_p) and the second comprising QA12+TMXDI (20(QA12+TMXDI)_p). The results were subjected to a comparative analysis of the properties of the standard dental copolymer consisting of UDMA 40 wt.%, Bis-GMA 40 wt.%, and TEGDMA 20 wt.% (40(UDMA)_p).

The novelty of this work combines the development of two new urethane-dimethacrylate monomers with quaternary ammonium groups (QAUDMAs) and the complex physicochemical, mechanical, and antibacterial characteristics of their copolymers with common dimethacrylates used in dentistry. So far, QAUDMAs synthesized from 1,3-bis(1-isocyanato-1-methylethyl)benzene have not been described in the literature.

The development of such materials is very important for dental science and may contribute to reducing the scale of dental carries in the future.

2. Materials and Methods

2.1. Materials

Bisphenol A-glycidyl dimethacrylate (Bis-GMA), triethylene glycol dimethacrylate (TEGDMA), urethane-dimethacrylate (UDMA), 1,3-bis(1-isocyanato-1-methylethyl)benzene (TMXDI), phenothiazine (PTZ), camphorquinone (CQ), *N,N*-dimethylaminoethyl methacrylate (DMAEMA), potassium bromide (KBr, FT-IR grade), and tetramethylsilane (TMS) were purchased from Sigma-Aldrich, St. Louis, MO, USA. Methyl methacrylate (MMA), *N*-methyl-diethanolamine (MDEA), decyl bromide (DB), and dodecyl bromide (DDB) were purchased from Acros Organics, Geel, Belgium. Dibutyltin dilaurate (DBTDL) was purchased from Fluka, Charlotte, NC, USA. Deuterated chloroform (CDCl_3) and deuterated dichloromethane (CD_2Cl_2) were purchased from Deutero GMBH, Kastellaun, Germany. Potassium carbonate (K_2CO_3), and magnesium sulfate (MgSO_4) were purchased from Chempur, Piekary Śląskie, Poland. Toluene, chloroform, and dichloromethane were purchased from Stanlab, Lublin, Poland. All chemicals were used as received.

2.2. Chemical Syntheses

2.2.1. *N,N*-(2-Hydroxyethyl)methylaminoethyl Methacrylate (HAMA)

The transesterification reaction reagents—MMA 1.00 mol (100.12 g), and MDEA 0.67 mol (79.85 g), the catalyst— K_2CO_3 8 wt.% (14.40 g), the polymerization inhibitor—PTZ 0.05% (0.09 g) and the solvent—toluene 400 cm³ were introduced into a single-necked round-bottom flask equipped with a Vigreux column and distillation head. The reaction mixture was brought to a boil. The equilibrium of the reaction was moved in favor of HAMA by the continuous collection of a distillate consisting of an azeotropic mixture of methanol (condensation reaction by-product), MMA (used in excess), and toluene (solvent). The reaction was carried out until the temperature at the column head reached 100 °C, which was achieved after 2.5 h. The cooled reaction mixture was filtered and washed three times with distilled water in a 1:2 volume ratio (HAMA and MDEA were soluble in water). The aqueous fractions were combined and extracted three times with chloroform in a 1:3 volume ratio (only HAMA was soluble in chloroform; as MDEA was water-insoluble, it remained in a water fraction). The chloroform fractions, containing only HAMA, were also combined, dried with MgSO_4 overnight, and chloroform was evaporated on a rotary evaporator under reduced pressure (30 and then 3 mbar). The obtained raw product was subjected to vacuum distillation (3 mbar), collecting a boiling fraction from 110 to 130 °C. The process yielded HAMA 14%.

2.2.2. 2-(Methacryloyloxy)ethyl-2-hydroxyethylmethylalkylammonium Bromides (QAHAMA-*n*, Where *n* Is the Number of Carbon Atoms in the *N*-Alkyl Substituent)

The Menshutkin reaction reagents—HAMA 0.107 mol (20.00 g), and alkyl bromide 0.107 mol (DB 23.66 g and DDB 26.67 g), and the polymerization inhibitor—PTZ 0.05 wt.% (0.022 and 0.023 g, respectively, in the reaction with DB and DDB) were introduced into a three-necked round-bottom flask equipped with a mechanical stirrer, reflux condenser, and thermometer. The reaction was carried out at 80 °C for 90 h. The reaction yielded 100% of 2-(methacryloyloxy)ethyl-2-decylhydroxyethylmethylammonium bromide (QAHAMA-10) and 2-(methacryloyloxy)ethyl-2-dodecylhydroxyethylmethylammonium bromide (QAHAMA-12).

2.2.3. Quaternary Ammonium Urethane-Dimethacrylates (QAUDMA)

A 50% solution of an addition reaction reagent—QAHAMA-*n* 0.070 mol (QAHAMA-10 28.50 g and QAHAMA-12 28.6 g), a catalyst—DBTDL 0.035 wt.% (0.013 g) and a solvent—dichloromethane 21 cm³ were introduced into a three-necked round-bottom flask equipped with a reflux condenser, thermometer, and dropping funnel. A 50% solution of the second

reagent, composed of TMXDI 0.035 mol (8.55 g) and dichloromethane 6.5 cm³, was placed in a dropping funnel. The flask content was brought to a boil (approximately 42 °C), and then a TMXDI solution was added dropwise for 1.5 h. The reaction was carried out for 5 h, maintaining the reaction mixture at the boiling point. Dichloromethane was evaporated on a rotary evaporator under reduced pressure (30 and then 3 mbar). A light-yellow, viscous, liquid substance remained in the flask, constituting the product. The flask with the product was placed in the laboratory dryer (SLW 53 STD, POL-EKO, Wodzisław Śląski, Poland) and heated at 42 °C for 24 h. The reaction yielded 100% both QAUDMAs, i.e., the addition reaction of TMXDI and QAHAMA-10 yielded QA10+TMXDI, and that of QAHAMA-12 yielded QA12+TMXDI.

2.3. Curing Procedure and Sample Preparation

Two experimental monomer compositions were prepared using mechanical stirring at 50 °C. They consisted of QAUDMA (QA10+TMXDI and QA12+TMXDI) 20 wt.%, UDMA 20 wt.%, Bis-GMA 40 wt.%, and TEGDMA 20 wt.%. The reference composition consisted of UDMA 40 wt.%, Bis-GMA 40 wt.%, and TEGDMA 20 wt.%. The components of the initiating system, comprising CQ 0.4 wt.% and DMAEMA 1 wt.%, were introduced into homogeneous monomer mixtures and stirring was continued at the same temperature until CQ dissolved. The achieved compositions were poured into the molds, covered with the PET foil, and irradiated with the UV-VIS lamp (Ultra Vitalux 300, Osram, Munich, Germany) at room temperature for 1 h. The lamp emitted radiation in the range of 280 to 780 nm and radiation exitance of 2400 mW/cm². The achieved casts were processed following the guidelines for specimen preparation for testing particular properties. Each specimen was polished with fine sandpaper before experiments.

2.4. Nuclear Magnetic Resonance Spectroscopy (NMR)

The NMR 300 MHz spectrometer (UNITY/INOVA, Varian, Palo Alto, CA, USA) was used to collect 256 scan ¹H spectra and 40,000 scan ¹³C NMR spectra of products achieved. CD₂Cl₂ and CDCl₃ were used as solvents and TMS was used as an internal standard.

2.5. Fourier Transform Infrared Spectroscopy (FTIR)

The FTIR spectrometer (Spectrum Two, Perkin-Elmer, Waltham, MA, USA) was used to collect spectra (128 scans, 1 cm⁻¹ resolution).

Monomers were tested as a very thin layer between two KBr pellets. Copolymers were powdered, sieved to a diameter of less than 25 μm, and dispersed in KBr pellets.

The degree of conversion (DC) in copolymers was calculated from the following equation:

$$DC = 1 - \frac{\left(\frac{A_{C=C}}{A_{Ar}}\right)_{polymer}}{\left(\frac{A_{C=C}}{A_{Ar}}\right)_{monomer}} \quad (1)$$

The variables in the equation are defined as follows:

$A_{C=C}$ —the absorbance of the stretching vibration band of the carbon–carbon double bond in the methacrylate group at 1636 cm⁻¹;

A_{Ar} —the absorbance of the aromatic stretching skeletal vibrations band at 1608 cm⁻¹.

2.6. Viscosity

The rotating viscometer (Visco Star Plus L, Brookfield Fungilab Viscometer, Barcelona, Spain) was used to determine the viscosity (η). The procedure was carried out at 25 °C according to the ISO 2555-2018 standard [43].

2.7. Refractive Index

The digital refractometer (DR 6100T, Krüss Optronic, Hamburg, Germany) was used to determine the refractive index (RI). The procedure was carried out according to the ISO 489:2022 standard [44].

2.8. Density and Polymerization Shrinkage

The density of monomers (d_m) was determined with the 1 mL pycnometer. The density of copolymers (d_p) was determined with the analytical balance (XP Balance, Mettler Toledo, Greifensee, Switzerland) analytical balance equipped with the density determination kit.

The polymerization shrinkage (S) was calculated from the following equation:

$$S(\%) = \left(1 - \frac{d_m}{d_p}\right) \times 100 \quad (2)$$

The variables in the equation are defined as follows:

d_m —the monomer density;

d_p —the polymer density.

2.9. Differential Scanning Calorimetry (DSC)

The differential scanning calorimeter (DSC 3, Mettler Toledo, Greifensee, Switzerland) was used in the measurements, utilizing powdered polymer samples and standard aluminum crucibles. The 10 K/min heating rate, 0 to 200 °C temperature range, and air atmosphere were used in all experiments.

The glass transition temperature (T_g) of copolymers was read off the DSC curve as the midpoint of the transition region, following the 11357-2:2020 standard [45].

2.10. Water Contact Angle

The goniometer (OCA 15EC, Data Physics, Filderstadt, Germany) was used to determine the water contact angle (WCA) of copolymer surfaces. The analysis was performed on disc-like specimens with dimensions of 15 mm × 1.5 mm (diameter × thickness) utilizing the sessile drop method and 4 µL of deionized water. The measurement was performed immediately after the drop was placed on the sample surface.

2.11. Water Sorption and Solubility

The water sorption (WS) and solubility (SL) of polymers were determined according to the guidelines of the ISO 4049:2019 standard [46] on disc-like specimens with dimensions of 15 mm × 1.5 mm (diameter × thickness). The analytical balance (XP Balance, Mettler Toledo, Greifensee, Switzerland) was used in experiments.

The specimens were dried to constant weight (m_0) in a laboratory dryer (SLW 53 STD, POL-EKO, Wodzisław Śląski, Poland) and immersed in deionized water at room temperature for 7 days. After that, samples were removed from the water, dried with blotting paper, weighed (m_1), and dried again to a constant weight (m_2).

WS and SL were calculated using the following equations:

$$WS \left(\frac{\mu\text{g}}{\text{mm}^3} \right) = \frac{m_1 - m_0}{V}, \quad (3)$$

$$SL \left(\frac{\mu\text{g}}{\text{mm}^3} \right) = \frac{m_0 - m_2}{V} \quad (4)$$

The variables in the equation are defined as follows:

m_0 —the initial mass of the dried samples;

m_1 —the mass of the swollen samples;

m_2 —the mass of the dried samples after immersion in water;

V —the initial volume of the dried samples.

2.12. Mechanical Properties

2.12.1. Hardness

The hardness tester (VEB, Werkstoffprüfmaschinen, Leipzig, Germany) was used to determine the ball indentation hardness (HB). The procedure was carried out according to the ISO 2039-1:2001 standard [47] on disc-like specimens with dimensions of 40 mm \times 4 mm (diameter \times thickness).

HB was calculated using the following equation:

$$HB \text{ (MPa)} = \frac{F_m \frac{0.21}{(h-h_r)+0.21}}{\pi d h_r} \quad (5)$$

The variables in the equation are defined as follows:

F_m —the test load;

d —the ball indenter diameter ($d = 5$ mm);

h —the immersion depth;

h_r —the reduced immersion depth ($h_r = 0.25$ mm).

2.12.2. Flexural Properties

The universal testing machine (Z020, Zwick, Ulm, Germany) was used to determine the flexural strength (FS) and flexural modulus (E). The procedure was carried out according to the ISO 178:2019 standard [48] on bar specimens with dimensions of 64 mm \times 10 mm \times 3.3 mm (length \times width \times thickness).

FS and E were calculated using the following equations:

$$FS \text{ (MPa)} = \frac{3Pl}{2bd^2}, \quad (6)$$

$$E \text{ (MPa)} = \frac{P_1 l^3}{4bd^3 \delta} \quad (7)$$

The variables in the equation are defined as follows:

P_1 —the load at the selected point of the elastic region of the stress–strain plot;

P —the maximum load;

l —the support span;

b —the sample width;

d —the sample thickness;

δ —the deflection of the sample at P_1 .

2.13. Antibacterial Properties

The antibacterial properties were characterized by the minimum bactericidal concentration (MBC) and minimum inhibitory concentration (MIC) against *S. aureus* (ATCC 25923) and *E. coli* (ATCC 25922). The tryptic soy broth (TSB) nutritious medium was used for the bacteria cultivation, which was carried out at 37 °C for 18 h in an incubator (ILW 53, POL-EKO, Wodzisław Śląski, Poland). The experiments were carried out on polymer powders sieved to a grain diameter of less than 25 μ m.

A series of six copolymer suspensions in TSB were prepared with concentrations of 50, 25, 12.5, 6.25, 3.125, and 1.563 mg/mL. Next, 20 μ L of *S. aureus* and *E. coli* bacterial suspensions in TSB ($\sim 5 \times 10^8$ CFU/mL) were introduced into the copolymer suspensions, vortexed (10 s, 2000 rpm), and incubated at 37 °C for 18 h. Suspensions were then vortexed again (10 s, 2000 rpm), and 100 μ L of each was applied on an agar plate (Müller-Hinton agar, Diag-Med, Raszyn, Poland). The agar plates were incubated at 37 °C for 18 h. The number of bacterial colonies was qualitatively assessed by visual comparison to the control. The lowest concentration at which no bacterial colonies were observed on agar plates was taken as the MBC . The lowest concentration at which the bacteria growth was reduced was taken as the MIC .

2.14. Statistical Analysis

The software (Statistica 13.3, TIBCO Software Inc., Palo Alto, CA, USA) was used to perform the non-parametric Wilcoxon test with a significance level (p) of 0.05. The statistical significance of the results was determined for five samples. The results were expressed as the average value (AV) and corresponding standard deviation (SD).

3. Results

3.1. Monomer Synthesis and Characterization

As part of this work, two QAUDMA monomers, QA10+TMXDI and QA12+TMXDI, were obtained. To achieve this goal, a procedure developed for the QAn+TMDI monomer synthesis was adopted [37].

The synthesis route of QA10+TMXDI and QA12+TMXDI included three stages (Figure 1):

- The transesterification of MMA with MDEA that led to HAMA formation. It was conducted with the MMA excess and K_2CO_3 catalyst;
- The Menshutkin reaction by the reaction of HAMA with DB and DDB resulted in a conversion of the HAMA tertiary amine group into a quaternary ammonium group in QAHAMA-n. QAHAMA-10 and QAHAMA-12 were achieved, respectively;
- The addition reaction of QAHAMA-n and TMXDI was conducted with the DBTDL catalyst and resulted in the formation of QAUDMAs: QA10+TMXDI and QA12+TMXDI;
- The chemical structure of the obtained monomers was confirmed using spectroscopic methods, including 1H NMR, ^{13}C NMR, and FTIR.

Figure 2 shows the 1H NMR spectra of the QA10+TMXDI and QA12+TMXDI monomers. Table 1 lists the proton signals present in the spectra with their assignment to chemical groups.

Table 1. 1H NMR signals of QA10+TMXDI and QA12+TMXDI monomers.

Signal Symbol	Hydrogen Atom	Multiplicity	Number of Protons	Chemical Shift [ppm]
a	$CH_3-C=$	s	6	1.95
b	$=CH_2$	2 m	4	5.70 and 6.14
c	$-O-CH_2-CH_2-N^+$	m	4	4.33–4.91
d	$-O-CH_2-CH_2-N^+$	m	4	4.00–4.26
e	$-N^+-CH_3$	s	6	3.30–3.77
f	$-O-CH_2-CH_2-N^+$	m	4	4.00–4.26
g	$-O-CH_2-CH_2-N^+$	m	4	4.33–4.91
h	$-NH-C=O$	m	2	7.10–7.80
i	$-N^+-CH_2-CH_2-(CH_2)_{7(or\ 9)}-CH_3$ ¹	m	4	3.30–3.77
j	$-N^+-CH_2-CH_2-(CH_2)_{7(or\ 9)}-CH_3$ ¹	m	4	1.49–1.88
k	$-N^+-CH_2-CH_2-(CH_2)_{7(or\ 9)}-CH_3$ ¹	m	28/36 ²	1.16–1.47
l	$-N^+-CH_2-CH_2-(CH_2)_{7(or\ 9)}-CH_3$ ¹	m	6	0.82–1.00
m	CH_3-C-CH_3	m	12	1.49–1.88
n	$-CH-$ (Ar)	m	1	7.10–7.80
o	$-CH-$ (Ar)	m	2	7.10–7.80
p	$-CH-$ (Ar)	m	1	7.10–7.80

¹ $-N^+-CH_2-CH_2-(CH_2)_7-CH_3$ corresponds to QA10+TMXDI, and $-N^+-CH_2-CH_2-(CH_2)_9-CH_3$ corresponds to QA12+TMXDI. ² 28 corresponds to QA10+TMXDI, and 36 corresponds to QA12+TMXDI.

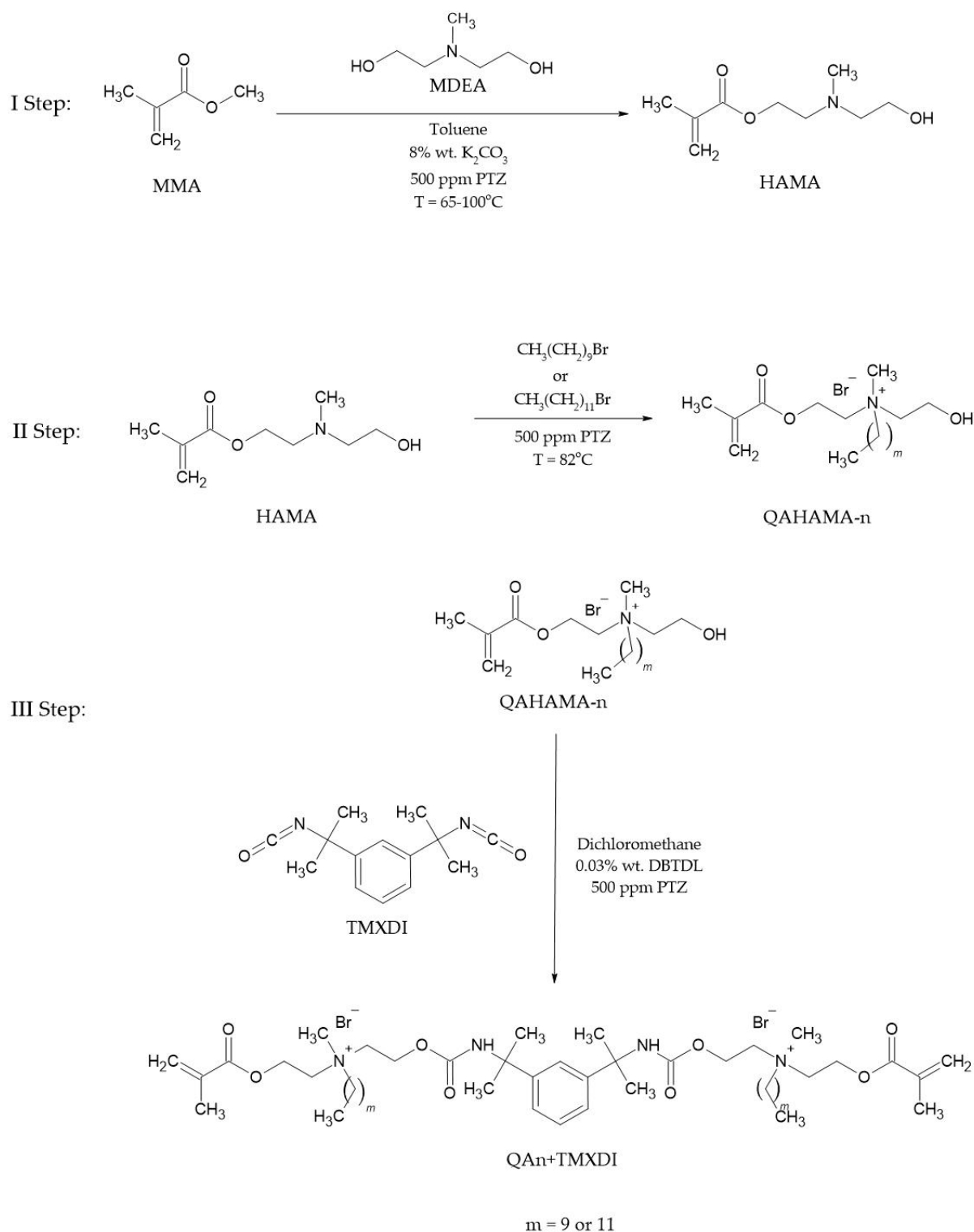


Figure 1. The synthesis route of QAUDMA monomers, namely QA10+TMXDI and QA12+TMXDI.

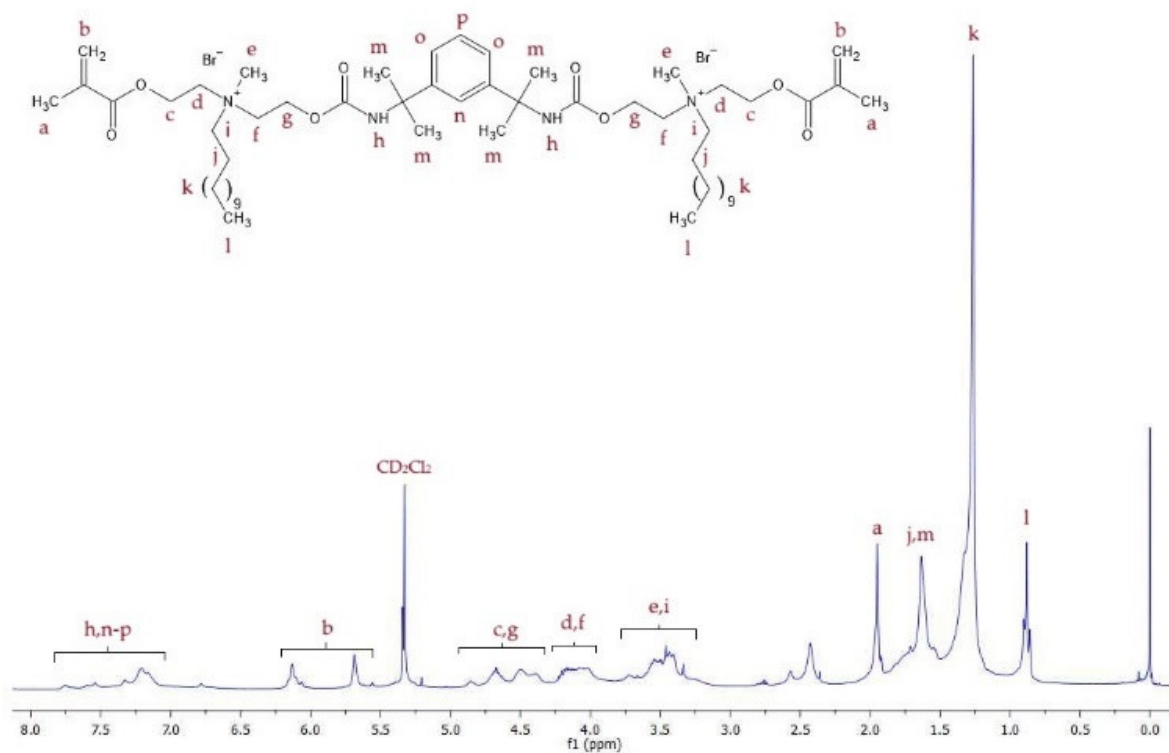
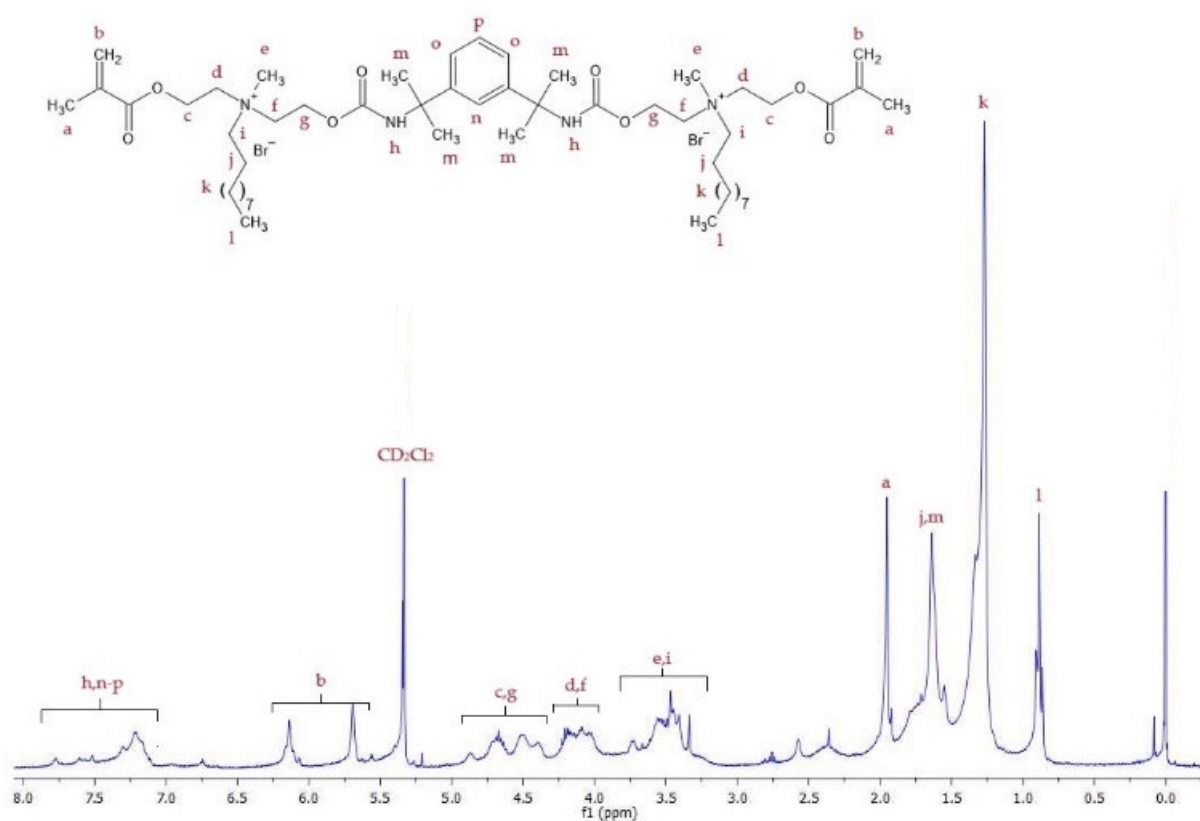
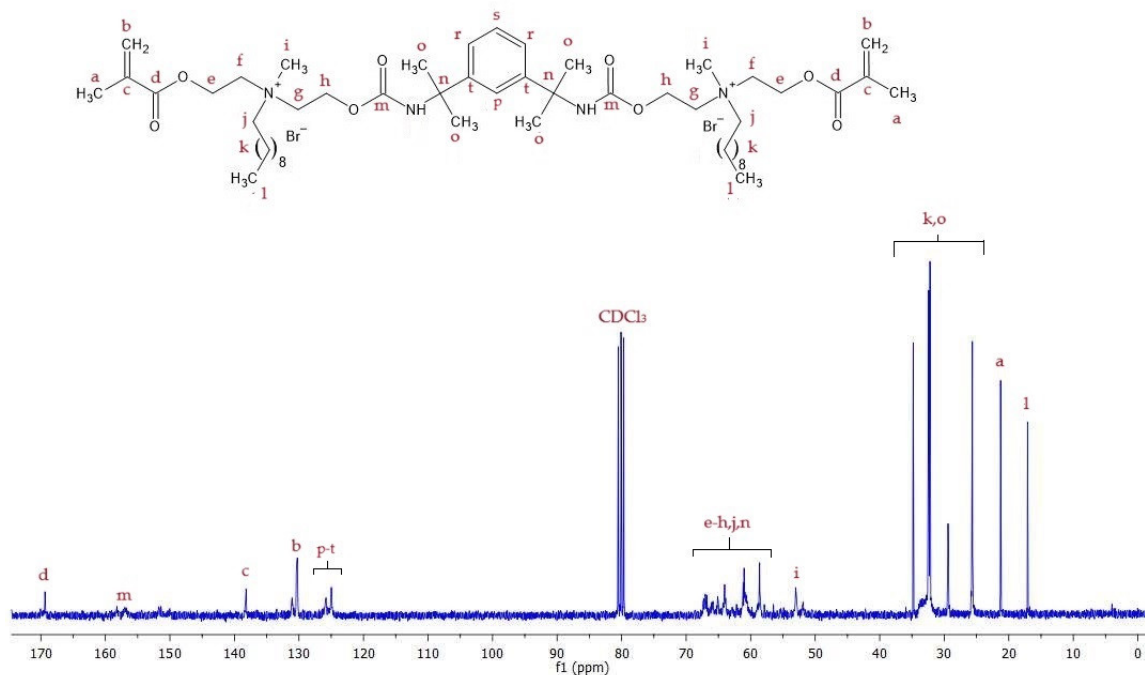
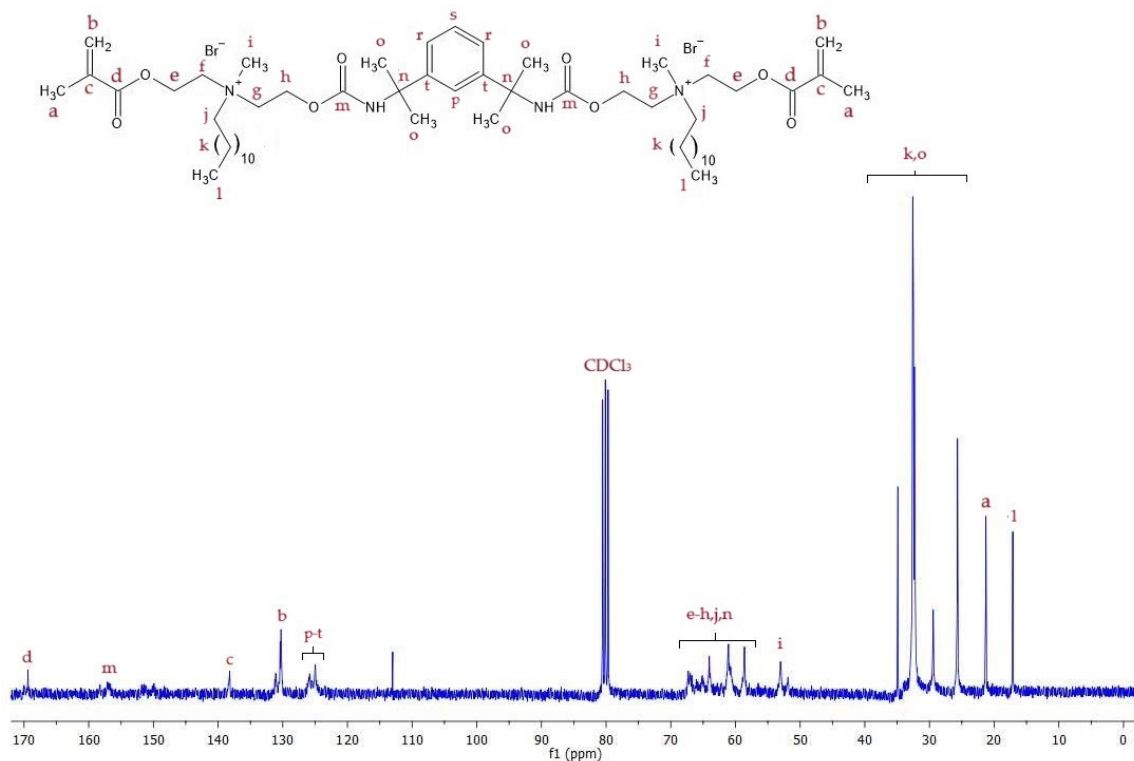


Figure 2. ^1H NMR spectra of monomers: (a) QA10+TMXDI; (b) QA12+TMXDI.

Figure 3 shows the ^{13}C NMR spectra of the QA10+TMXDI and QA12+TMXDI monomers. Table 2 lists carbon atom signals present in the spectra with their assignment to chemical groups.



(a)



(b)

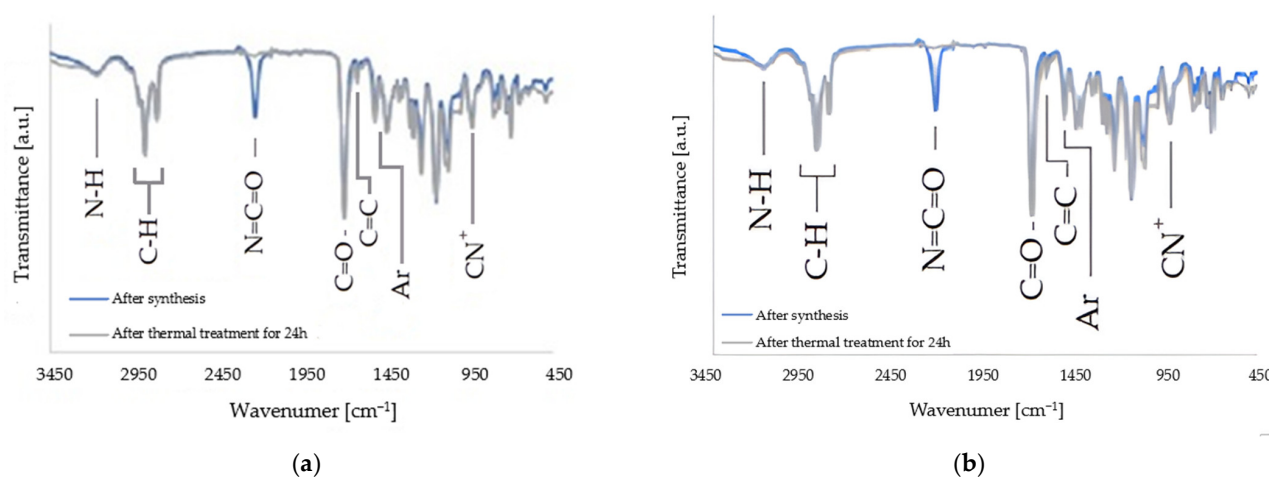
Figure 3. ^{13}C NMR spectra of monomers: (a) QA10+TMXDI; (b) QA12+TMXDI.

Table 2. ^{13}C NMR signals of QA10+TMXDI and QA12+TMXDI monomers.

Signal Symbol	Carbon Atom	Chemical Shift [ppm]
a	$\text{CH}_3\text{-C=}$	21
b	=CH_2	130
c	$\text{CH}_3\text{-C=CH}_2$	138
d	-O-C=O	169
e-h	$\text{-CH}_2\text{-}$	59–67
i	$\text{-N}^+\text{-CH}_3$	53
j	$\text{-N}^+\text{-CH}_2\text{-(CH}_2\text{)}_{8(\text{or } 10)\text{-CH}_3$ ¹	59–67
k	$\text{-N}^+\text{-CH}_2\text{-(CH}_2\text{)}_{8(\text{or } 10)\text{-CH}_3$ ¹	26–35
l	$\text{-N}^+\text{-CH}_2\text{-(CH}_2\text{)}_{8(\text{or } 10)\text{-CH}_3$ ¹	17
m	-NH-C=O	157
n	-NH-C-	59–67
o	>C-CH_3	26–35
p-s	-CH= (Ar)	124–126
t	>C= (Ar)	124–126

¹ $\text{-N}^+\text{-CH}_2\text{-(CH}_2\text{)}_8\text{-CH}_3$ corresponds to QA10+TMXDI, and $\text{-N}^+\text{-CH}_2\text{-(CH}_2\text{)}_{10}\text{-CH}_3$ corresponds to QA12+TMXDI.

Figure 4 shows the FTIR spectra of the QA10+TMXDI and QA12+TMXDI monomers. Table 3 lists of absorption bands present in the spectra with their assignment to chemical groups.

**Figure 4.** FTIR spectra of the achieved QAUDMA monomers: (a) QA10+TMXDI; (b) QA12+TMXDI.**Table 3.** The interpretation of FTIR spectra of QA10+TMXDI and QA12+TMXDI monomers.

Chemical Bond	Intensity ¹	Wavenumber [cm ⁻¹]
N-H	w	3215
CH ₃	w	3024
=CH ₂	m	2957
CH ₂ , CH ₃	m	2925 and 2855
N=C=O ²	s	2257
C=O	s	1714
C=C	w	1638
C=C (Ar)	w	1605
NH (urethane)	m	1529
CH ₂ , CH ₃	m	1457
C-N	m	1249 and 1158
C-O-C	m	1092 and 1087
C-N ⁺	m	943

¹ The intensity of the absorption bands in the FTIR spectra was referred to as strong (s), medium (m), and weak (w). ² Refers to the isocyanate group absorption band present in the FTIR spectra of the QAUDMA monomers before their thermal treatment.

The QA10+TMXDI and QA12+TMXDI monomers were characterized by their molecular weight (MW), concentration of double bonds (x_{DB}), refractive index (RI), and density (d_m). Table 4 presents the results for the experimental monomers and three commercial dental dimethacrylate monomers (Bis-GMA, UDMA, and TEGDMA), for comparison.

Table 4. Properties of QA10+TMXDI and QA12+TMXDI related to properties of Bis-GMA, UDMA, and TEGDMA. The lowercase letter “a” in the superscripts indicate couples with statistically significant results ($p \leq 0.05$). The remaining results did not have statistical significance ($p > 0.05$).

Monomer Name	MW (g/mol)	x_{DB} (mol/kg)	RI	d_m (g/cm ³)
			AV ¹	AV ²
Experimental monomers				
QA10+TMXDI	1061	1.89	1.5230	1.16 ^a
QA12+TMXDI	1117	1.79	1.5138	1.33 ^a
Reference monomers				
Bis-GMA	512	3.90	1.5493 ³	1.15 ³
UDMA	470	4.25	1.4614 ³	1.09 ³
TEGDMA	286	6.99	1.4852 ³	1.07 ³

¹ The SD for the RI values was 0.0001. ² The SD for the d_m values was 0.01. ³ Taken from [37].

The molecular weight (MW) of QA10+TMXDI was 1061 g/mol and QA12+TMXDI had a MW that was 5% higher. Compared to Bis-GMA, UDMA, and TEGDMA, QA10+TMXDI as well as QA12+TMXDI had a higher MW , on average by 53, 57, and 74%, respectively. The MW was converted to the concentration of double bonds (x_{DB}). The x_{DB} of QA10+TMXDI was 1.89 mol/kg and QA12+TMXDI had a x_{DB} that was 5% lower. Compared to Bis-GMA, UDMA, and TEGDMA, QA10+TMXDI as well as QA12+TMXDI had a lower x_{DB} , on average by 53, 57, and 74%, respectively.

The refractive index (RI) of QA10+TMXDI was 1.5230 and QA12+TMXDI had a RI that was 0.6% lower. This difference did not have statistical significance. Compared to Bis-GMA, QA10+TMXDI as well as QA12+TMXDI had a lower RI , on average by 2%. Compared to UDMA and TEGDMA, QA10+TMXDI as well as QA12+TMXDI had a higher RI , on average by 4 and 3%, respectively.

The density (d_m) of QA10+TMXDI was 1.16 g/cm³ and QA12+TMXDI had a d_m that was 15% higher. This difference was statistically significant. Compared to Bis-GMA, UDMA, and TEGDMA, QA10+TMXDI as well as QA12+TMXDI had a higher d_m . In the case of QA10+TMXDI, these differences were 1, 7, and 9%, respectively, for Bis-GMA, UDMA, and TEGDMA. In the case of QA12+TMXDI, these differences were greater and equaled 16, 22, and 25%, respectively, for Bis-GMA, UDMA, and TEGDMA.

3.2. Characterization of Monomer Compositions

The obtained QA10+TMXDI and QA12+TMXDI monomers were used to prepare compositions with commercial DMA monomers. QAUDMA 20 wt.% was mixed with UDMA 20 wt.%, Bis-GMA 40 wt.%, and TEGDMA 20 wt.%. For comparison purposes, the UDMA 40 wt.%, Bis-GMA 40 wt.%, and TEGDMA 20 wt.% mixture was prepared. Table 5 shows the names, weight, and molar ratios of the prepared monomer compositions.

The 20(QA10+TMXDI)_m and 20(QA12+TMXDI)_m experimental monomer compositions and 40(UDMA)_m reference monomer composition were characterized by their molecular weight (MW), concentration of double bonds (x_{DB}), viscosity (η), refractive index (RI), and density (d_m). Table 6 lists the values of these parameters.

Table 5. Compositions of QAUDMA, Bis-GMA, UDMA, and TEGDMA experimental mixtures related to the Bis-GMA, UDMA, and TEGDMA reference mixture.

Monomer Composition	Sample Composition							
	QAUDMA		UDMA		Bis-GMA		TEGDMA	
	Mass Fraction	Mole Fraction	Mass Fraction	Mole Fraction	Mass Fraction	Mole Fraction	Mass Fraction	Mole Fraction
Experimental compositions								
20(QA10+TMXDI) _m	0.20	0.09	0.20	0.20	0.40	0.37	0.20	0.34
20(QA12+TMXDI) _m	0.20	0.09	0.20	0.20	0.40	0.37	0.20	0.34
Reference composition								
40(UDMA) _m	0.00	0.00	0.40	0.36	0.40	0.34	0.20	0.30

Table 6. Properties of 20(QA10+TMXDI)_m and 20(QA12+TMXDI)_m experimental monomer compositions related to properties of the 40(UDMA)_m reference monomer composition. The lowercase letters “a” and “b” in the superscripts indicate couples with statistically significant results ($p \leq 0.05$). The remaining results did not have statistical significance ($p > 0.05$).

Monomer Composition	MW (g/mol)	x_{DB} (mol/kg)	η (Pa·s)		RI	d_m (g/cm ³)
			AV	SD	AV ¹	AV ²
Experimental compositions						
20(QA10+TMXDI) _m	476	4.20	3.79	0.40	1.5101	1.13 ^{a,b}
20(QA12+TMXDI) _m	481	4.16	3.22	0.30	1.5094	1.11 ^a
Reference composition						
40(UDMA) _m	429	4.66	3.53	0.40	1.5049	1.11 ^b

¹ The SD for the RI values always was 0.0001. ² The SD for the d_m values was always 0.01.

The MW of 20(QA10+TMXDI)_m was 476 g/mol and 20(QA12+TMXDI)_m had a MW that was 1% higher. Compared to 40(UDMA)_m, 20(QA10+TMXDI)_m as well as 20(QA12+TMXDI)_m had a higher MW, by 10 and 11%, respectively. The MW was converted to the concentration of double bonds in the monomer compositions. The x_{DB} of 20(QA10+TMXDI)_m was 4.20 mol/kg and 20(QA12+TMXDI)_m had a x_{DB} that was 1% lower. Compared to 40(UDMA)_m, 20(QA10+TMXDI)_m as well as 20(QA12+TMXDI)_m had a lower x_{DB} , by 10 and 11%, respectively.

The η of 20(QA10+TMXDI)_m was 3.79 Pa·s and 20(QA12+TMXDI)_m had a 15% lower η . Compared to 40(UDMA)_m, 20(QA10+TMXDI)_m had a higher η , whereas 20(QA12+TMXDI)_m had a lower η , by 7 and 9%, respectively. All these differences did not have statistical significance.

The RI of 20(QA10+TMXDI)_m was 1.5101 and 20(QA12+TMXDI)_m had a RI that was 0.05% higher. Compared to 40(UDMA)_m, 20(QA10+TMXDI)_m as well as 20(QA12+TMXDI)_m had a higher RI, by 0.30 and 0.35%. All these differences did not have statistical significance.

The d_m of 20(QA10+TMXDI)_m was 1.13 g/cm³ and 20(QA12+TMXDI)_m had a d_m that was 2% lower. This difference was statistically significant. Compared to 40(UDMA)_m, 20(QA10+TMXDI)_m had a d_m that was 2% lower, and this difference was statistically significant, whereas 20(QA12+TMXDI)_m had the same d_m , and this result did not have statistical significance.

3.3. Characterization of Copolymers

20(QA10+TMXDI)_m, 20(QA12+TMXDI)_m, and 40(UDMA)_m were subjected to photopolymerization, utilizing an initiation system consisting of CQ and DMAEMA, which is typical for the DCRM photocuring. The structure of the obtained copolymers was characterized by the degree of conversion (DC). The physical properties were characterized by determining the polymerization shrinkage (S), glass transition temperature (T_g), wa-

ter sorption (*WS*), water solubility (*SL*), and water contact angle (*WCA*). The mechanical properties were characterized by determining the hardness (*HB*), flexural modulus (*E*), and flexural strength (*FS*). The copolymers were also tested for antibacterial properties by determining the minimum bactericidal concentration (*MBC*) and minimum inhibitory concentration (*MIC*) against *S. aureus* (ATCC 25923) and *E. coli* (ATCC 25922).

3.3.1. Degree of Conversion (*DC*)

The *DC* was determined utilizing the FTIR spectroscopy and internal standard method. As the tested systems comprised the TMXDI moiety, it was possible to use the aromatic skeletal vibration band as a standard (Figure 5). This is the most widely used method in the *DC* characterization of poly(dimethacrylate)s because this band does not change its specificity due to polymerization [49]. Table 7 shows the *DC* in the copolymers tested.

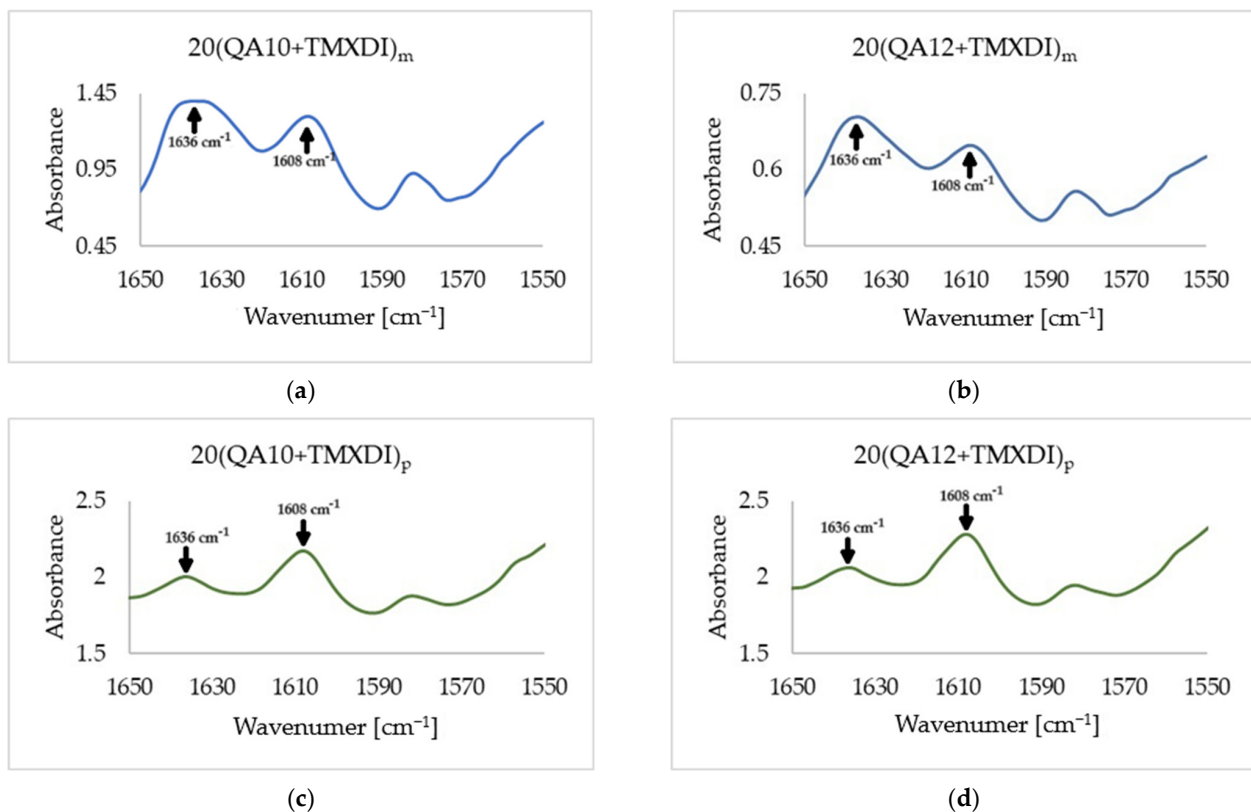


Figure 5. FTIR spectra showing the disappearance of the absorption band of the C=C stretching vibrations at 1636 cm^{-1} due to polymerization, and the absorption band of the aromatic stretching skeletal vibrations at 1608 cm^{-1} , which was used as an internal standard: (a) $20(\text{QA}10+\text{TMXDI})_m$; (b) $20(\text{QA}12+\text{TMXDI})_m$; (c) $20(\text{QA}10+\text{TMXDI})_p$; and (d) $20(\text{QA}12+\text{TMXDI})_p$.

Table 7. The *DC* in copolymers. The lowercase letters “a” and “b” in the superscripts indicate couples with statistically significant results ($p \leq 0.05$). The remaining results did not have statistical significance ($p > 0.05$).

Copolymer	<i>DC</i>	
	<i>AV</i>	<i>SD</i>
Experimental copolymers		
$20(\text{QA}10+\text{TMXDI})_p$	0.57 ^a	0.05
$20(\text{QA}12+\text{TMXDI})_p$	0.69 ^{a,b}	0.06
Reference copolymer		
$40(\text{UDMA})_p$	0.54 ^b	0.04

The DC in $20(QA10+TMXDI)_p$ was 0.57 and $20(QA12+TMXDI)_p$ had a DC that was 21% higher. This difference was statistically significant. Compared to $40(UDMA)_p$, $20(QA10+TMXDI)_p$ as well as $20(QA12+TMXDI)_p$ had a higher DC , by 6 and 28%, respectively. The difference for $20(QA10+TMXDI)_p$ was statistically insignificant, whereas that for $20(QA12+TMXDI)_p$ was statistically significant.

3.3.2. Physical Properties

Table 8 shows the results obtained for the d_p , S , and T_g of the copolymers tested. The DSC thermograms of the copolymers are presented in Supplementary Materials in Figure S1.

Table 8. The physical properties of copolymers: density (d_p), polymerization shrinkage (S), and glass transition temperature (T_g). The lowercase letters “a”–“c” in the superscripts indicate couples with statistically significant results ($p \leq 0.05$). The remaining results did not have statistical significance ($p > 0.05$).

Copolymer	d_p (g/cm ³)		S (%)		T_g (°C)	
	AV	SD	AV	SD	AV	SD
Experimental copolymers						
$20(QA10+TMXDI)_p$	1.21	0.01	7.04 ^{a,b}	0.83	53.46 ^{a,b}	3.27
$20(QA12+TMXDI)_p$	1.20	0.01	7.72 ^{a,c}	1.17	60.30 ^a	4.34
Reference copolymer						
$40(UDMA)_p$	1.20	0.01	7.42 ^{b,c}	1.08	62.97 ^b	4.52

The d_p of $20(QA10+TMXDI)_p$ was 1.21 g/cm³ and $20(QA12+TMXDI)_p$ had a d_p that was 1% lower. Compared to $40(UDMA)_p$, $20(QA10+TMXDI)_p$ had a higher d_p , by 1%, whereas $20(QA12+TMXDI)_p$ had the same d_p . All the results for the d_p were statistically insignificant.

The S of $20(QA10+TMXDI)_p$ was 7.04% and the S of $20(QA12+TMXDI)_p$ was 10% higher. Compared to $40(UDMA)_p$, $20(QA10+TMXDI)_p$ had a lower S , whereas $20(QA12+TMXDI)_p$ had a higher S , by 5 and 4%, respectively. All these differences were statistically significant.

The T_g of $20(QA10+TMXDI)_p$ was 53.46 °C and $20(QA12+TMXDI)_p$ had a T_g that was 13% higher. This difference was statistically significant. Compared to $40(UDMA)_p$, $20(QA10+TMXDI)_p$ as well as $20(QA12+TMXDI)_p$ had a lower T_g , by 15 and 4%, respectively. The difference for $20(QA10+TMXDI)_p$ was statistically significant. The other copolymer did not have statistical significance.

Table 9 shows the results obtained for the WS , SL , and WCA of the tested copolymers. The goniometry camera images of the deionized water droplets on the surfaces of the copolymers are presented in Supplementary Materials in Figure S2.

Table 9. The physical properties characterizing copolymers’ interaction with water: water sorption (WS), water leachability (SL), and water contact angle (WCA). The lowercase letters “a”–“c” in the superscripts indicate couples with statistically significant results ($p \leq 0.05$). The remaining results did not have statistical significance ($p > 0.05$).

Copolymer	WS (µg/mm ³)		SL (µg/mm ³)		WCA (°)	
	AV	SD	AV	SD	AV	SD
Experimental copolymers						
$20(QA10+TMXDI)_p$	10.43 ^a	0.42	2.18 ^{a,b}	0.06	87.03 ^a	3.07
$20(QA12+TMXDI)_p$	10.35 ^b	0.23	2.46 ^{a,c}	0.25	91.30 ^b	4.82
Reference copolymer						
$40(UDMA)_p$	5.31 ^{a,b}	0.36	0.17 ^{b,c}	0.09	74.07 ^{a,b}	2.24

The *WS* of 20(QA10+TMXDI)_p was 10.43 µg/mm³ and 20(QA12+TMXDI)_p had a *WS* that was 1% higher. This difference was statistically insignificant. Compared to 40(UDMA)_p, 20(QA10+TMXDI)_p as well as 20(QA12+TMXDI)_p had a higher *WS*, by 96 and 95%, respectively. These differences were statistically significant.

The *SL* of 20(QA10+TMXDI)_p was 2.18 µg/mm³ and 20(QA12+TMXDI)_p had a *SL* that was 13% higher. Compared to 40(UDMA)_p, 20(QA10+TMXDI)_p as well as 20(QA12+TMXDI)_p had a higher *SL*, by 1182 and 1347%, respectively. All these differences were statistically significant.

The *WCA* of 20(QA10+TMXDI)_p was 87.03° and 20(QA12+TMXDI)_p had a *WCA* that was 5% higher. This difference was statistically insignificant. Compared to 40(UDMA)_p, 20(QA10+TMXDI)_p as well as 20(QA12+TMXDI)_p had a higher *WCA*, by 17 and 23%, respectively. These differences were statistically significant.

3.3.3. Mechanical Properties

Table 10 shows the results obtained for the *HB*, *E*, and *FS* of the tested copolymers.

Table 10. The mechanical properties of copolymers: hardness (*HB*), flexural modulus (*E*), and flexural strength (*FS*). The lowercase letters “a”–“c” in the superscripts indicate couples with statistically significant results ($p \leq 0.05$). The remaining results did not have statistical significance ($p > 0.05$).

Copolymer	<i>HB</i> (MPa)		<i>FS</i> (MPa)		<i>E</i> (MPa)	
	<i>AV</i>	<i>SD</i>	<i>AV</i>	<i>SD</i>	<i>AV</i>	<i>SD</i>
Experimental copolymers						
20(QA10+TMXDI) _p	234.8 ^{a,b}	8.7	100.6 ^a	11.7	3244.9 ^a	114.1
20(QA12+TMXDI) _p	194.6 ^{a,c}	26.5	90.3 ^b	6.1	3020.6 ^b	198.9
Reference copolymer						
40(UDMA) _p	225.9 ^{b,c}	19.4	125.4 ^{a,b}	13.0	3597.7 ^{a,b}	154.4

The *HB* of 20(QA10+TMXDI)_p was 234.8 MPa and 20(QA12+TMXDI)_p had a *HB* that was 17% lower. Compared to 40(UDMA)_p, 20(QA10+TMXDI)_p had a *HB* that was 4% higher, and 20(QA12+TMXDI)_p had a *HB* that was 14% lower. All these differences were statistically significant.

The *FS* of 20(QA10+TMXDI)_p was 100.63 MPa and 20(QA12+TMXDI)_p had a *FS* that was 10% lower. This difference was not statistically significant. Compared to 40(UDMA)_p, 20(QA10+TMXDI)_p and 20(QA12+TMXDI)_p had a lower *FS*, by 20 and 28%, respectively. These differences were statistically significant.

The *E* of 20(QA10+TMXDI)_p was 3244.9 MPa and 20(QA12+TMXDI)_p had a *E* that was 7% lower. This difference was not statistically significant. Compared to 40(UDMA)_p, 20(QA10+TMXDI)_p and 20(QA12+TMXDI)_p had a lower *E*, by 10 and 16%, respectively. These differences were statistically significant.

3.3.4. Antibacterial Properties

Table 11 shows the results obtained for the *MIC* and *MBC* of the tested copolymers concerning the *S. aureus* (ATCC 25923) and *E. coli* (ATCC 25922) bacteria strains. The results of the experiments are presented in Supplementary Materials in Figures S3–S8.

20(QA10+TMXDI)_p had an *MBC* of 12.5 mg/mL, and an *MIC* of 6.25 mg/mL concerning both bacteria tested. 20(QA12+TMXDI)_p had an *MBC* as well as *MIC* greater than 50 mg/mL concerning *S. aureus*. The same copolymer showed a lower *MBC* and *MIC* concerning *E. coli*, respectively, 25 and 12.5 mg/mL. 40(UDMA)_p had an *MBC* as well as *MIC* greater than 50 mg/mL in each case, i.e., concerning both bacteria strains.

Table 11. The antibacterial properties of copolymers against *S. aureus* (ATCC 25923) and *E. coli* (ATCC 25922): minimum bactericidal concentration (MBC) and minimum inhibitory concentration (MIC).

Copolymer	MBC [mg/mL]		MIC [mg/mL]	
	<i>S. aureus</i> (ATCC 25923)	<i>E. coli</i> (ATCC 25922)	<i>S. aureus</i> (ATCC 25923)	<i>E. coli</i> (ATCC 25922)
Experimental copolymers				
20(QA10+TMXDI) _p	12.5	12.5	6.25	6.25
20(QA12+TMXDI) _p	>50	25	>50	12.5
Reference copolymer				
40(UDMA) _p	>50	>50	>50	>50
Control				
Sterile Water	-	-	-	-

4. Discussion

As part of this study, two novel urethane-dimethacrylate monomers with two QA groups were obtained. For this purpose, the methodology that we developed to obtain an analogous series of urethane-dimethacrylate monomers with two QA groups and a core derived from 1,6-diisocyanato-2,2,4-trimethylhexane (TMDI) was adopted (QAn+TMDI, where n describes the number of carbon atoms in the *N*-alkyl substituent) [37]. Qan+TMDIs were obtained in a three-step process in which HAMA, QAHAMA-*n*, and Qan+TMDI were successively synthesized. In this study, we used TMXDI instead of TMDI. TMXDI is classified as an aliphatic isocyanate, but it has a central 1,3-phenylene ring [50]. The addition reaction of QAHAMA-*n* and TMXDI resulted in the formation of QA10+TMXDI and QA12+TMXDI (Figure 1).

The spectroscopic analysis confirmed the chemical structure of the obtained monomers. The ¹H NMR (Figure 2, Table 1), as well as ¹³C NMR (Figure 3, Table 2) spectra of QA10+TMXDI and QA12+TMXDI, showed the presence of signals coming from the urethane linkage, TMXDI core, methacrylate group, MDEA moiety, and *N*-alkyl substituent. The signal locations of the -CH₃ and -CH₂- groups adjacent to the quaternary nitrogen were specific to the QA group neighborhood. Signals derived from the proton and carbon atoms of the -CH₃ group neighboring to N⁺ were found from 3.30 to 3.77 ppm in the ¹H NMR spectra and at 53 ppm in the ¹³C NMR spectra. In the ¹H NMR spectrum of HAMA, that -CH₃ group gives a singlet at a higher field, i.e., ca. 2.4 ppm. In the ¹³C NMR spectrum of HAMA, a signal derived from the -CH₃ group adjacent to N⁺ can be also found at a higher field, i.e., ca. 42 ppm [37]). The formation of the urethane linkage was confirmed by the presence of signals of the -NHCOO- proton, present in the range from 7.10 to 7.80 ppm in the ¹H NMR spectra, and the -NHCOO- carbon atom, present at 157 ppm in ¹³C NMR spectra. The quaternization and formation of the urethane linkage were additionally confirmed from the FTIR analysis. In the FTIR spectra, a band of the C-N⁺ bond vibrations was present at 943 cm⁻¹, whereas the C-N bond vibrations of the -NHCOO- linkage resulted in two bands at 3215 and 1529 cm⁻¹ (Figure 4, Table 3).

Physicochemical properties QA10+TMXDI and QA12+TMXDI depended on the *N*-alkyl substituent length (Table 4). Its extension with two methylene groups resulted in a 5% increase in the *MW* and *x*_{DB}. The *RI* decreased by 0.6% and the *d*_m increased by 15%.

QA10+TMXDI and QA12+TMXDI had a *MW* of 1061 and 1117 g/mol and a *x*_{DB} of 1.89 and 1.79 mol/kg, respectively (Table 4). This showed that the extension of the *N*-alkyl substituent with two methylene groups resulted in a 5% increase in the *MW* and the same decrease in the *x*_{DB}. The *Ris* of QA10+TMXDI and QA12+TMXDI were 1.5230 and 1.5138, respectively. This corresponded to the statistically insignificant decrease in the *RI* of 0.6% when the *N*-alkyl substituent length increased. The *d*_m increased from 1.16 to 1.33 g/cm³ with the increase in the *N*-alkyl substituent length. This was a 15% change, and this had statistical significance. It can be seen that the physicochemical properties of experimental

QAUDMAs depended on the *N*-alkyl substituent length. The more noticeable change was observed for density. The increase in density may suggest the tighter packing of the QA12+TMXDI molecule than that of QA10+TMXDI, regardless of whether it had longer *N*-alkyl substituents.

Compared to Bis-GMA, UDMA, and TEGDMA, QA10+TMXDI and QA12+TMXDI had a higher MW (Table 4). The MWs of QA10+TMXDI and QA12+TMXDI were approximately more than twice as much as Bis-GMA (512 g/mol) and UDMA (470 g/mol), and almost four times as much as TEGDMA (286 g/mol). This resulted in a lower x_{DB} of QA10+TMXDI (1.89 mol/kg) and QA12+TMXDI (1.79 mol/kg) compared to dental DMAs (3.90, 4.25, and 6.99 mol/kg, respectively, for Bis-GMA, UDMA, and TEGDMA [37]).

The light-bending ability of QA10+TMXDI and QA12+TMXDI was adequate for a DCRM matrix. Their *Ris* (respectively, 1.5230 and 1.5138) were very close to that of dental DMAs (1.5493, 1.4614, and 1.4852, respectively, for Bis-GMA, UDMA, and TEGDMA [37]) and were within the range of 1.46 to 1.55, which is recommended for dental systems [51,52].

The densities of QA10+TMXDI (1.16 g/cm³) and QA12+TMXDI (1.33 g/cm³) were higher than those of Bis-GMA, UDMA, and TEGDMA (1.15, 1.09, and 1.07 g/cm³, respectively [37]). If compared to fully aliphatic UDMA and TEGDMA, it is understandable that the synthesized QAUDMAs had a higher density, as the TMXDI benzene ring is heavy and capable of tight packing [53]. The comparison of the d_m of QA10+TMXDI and QA12+TMXDI to that of Bis-GMA showed that they had higher densities. Listing the important differences in the chemical structure of experimental QAUDMAs and Bis-GMA may be useful in explaining this observation:

- Bis-GMA has a more spacious core comprising two 1,4-phenylene rings, whereas QA10+TMXDI and QA12+TMXDI has one central 1,3-phenylene ring;
- Bis-GMA has shorter aliphatic wings than QA10+TMXDI and QA12+TMXDI;
- Bis-GMA provides a hydroxyl proton donor to the hydrogen bonds, whereas QA10+TMXDI and QA12+TMXD create these bonds involving the urethane proton donor group;
- QA10+TMXDI and QA12+TMXDI have two long *N*-alkyl substituents in the wings.

It can be concluded that the asymmetrical substitution in the central benzene ring and the long *N*-alkyl substituents do not disturb the tight packing of QA10+TMXDI and QA12+TMXDI.

The QA10+TMXDI and QA12+TMXDI monomers were introduced into the common DCRM dental dimethacrylate composition of UDMA 40 wt.%, Bis-GMA 40 wt.%, and TEGDMA 20 wt.%. The idea was to replace half of UDMA with one of the QAUDMAs, i.e., QA10+TMXDI and QA12+TMXDI. Correspondingly, the novel formulations comprised QAUDMA 20 wt.%, UDMA 20 wt.%, Bis-GMA 40 wt.%, and TEGDMA 20 wt.% (Table 5).

Only a negligible effect of the *N*-alkyl substituent on the 20(QA10+TMXDI)_m and 20(QA12+TMXDI)_m properties was observed (Table 6). The extension of the *N*-alkyl substituents by two methylene groups resulted in a 1% decrease in the x_{DB} , a 15% decrease in the η , a 0.05% increase in the *RI*, and a 2% increase in the d_m . These differences were statistically insignificant, except for the d_m , which was statistically significant. The most notable change occurred in the viscosity. Its decrease can suggest the weakening of intermolecular interactions in 20(QA12+TMXDI)_m caused by the *N*-dodecyl substituent [53].

Compared to 40(UDMA)_m, the experimental compositions had about a 10% higher MW and 10% lower x_{DB} . This suggests that the replacement of half of UDMA with one of QAUDMAs would have a minor impact on a decrease in the theoretical crosslink density of the resulting copolymer [54].

The comparison of 40(UDMA)_m and the experimental compositions by the viscosity, refractive index, and density also led to satisfactory conclusions. 40(UDMA)_m had the η of 3.53 Pa·s, which was in the range limited by the η of 20(QA10+TMXDI)_m and 20(QA12+TMXDI)_m, i.e., 3.79 and 3.22 Pa·s, respectively. In addition, differences in the η between 40(UDMA)_m and 20(QA10+TMXDI)_m or 20(QA12+TMXDI)_m were only 7 and 9%, respectively, and they did not have statistical significance. This showed that the experimental formulations

would have flowability similar to the reference formulation, which would be beneficial to the DCRM preparation. The transparency of 20(QA10+TMXDI)_m and 20(QA12+TMXDI)_m also was suitable for dental materials. Their *Ri*s were of 1.5101 and 1.5094, respectively. This matches the *RI* range of 1.46 to 1.55, which is recommended for dental materials [51,52]. In addition, the difference in the *RI* of the experimental compositions and reference composition was statistically insignificant. Finally, the *d_m* of 20(QA12+TMXDI)_m and 40(UDMA)_m had the same value of 1.11 g/cm³. 20(QA10+TMXDI)_m had a *d_m* that was 2% higher, and that difference was statistically significant.

20(QA10+TMXDI)_m and 20(QA12+TMXDI)_m were subjected to photopolymerization towards two experimental copolymers 20(QA10+TMXDI)_p and 20(QA12+TMXDI)_p. They were characterized by the *DC* as the fundamental parameter used to characterize the polymer network structure (Table 7). An appropriately high *DC* is responsible for the adequate physical and mechanical properties of the DCRM matrices and the effective functioning of a dental filling [55,56]. The *DC* of novel QAUDMAs increased statistically significantly with the extension of the *N*-alkyl substituent. 20(QA10+TMXDI)_p had a *DC* of 0.57 and 20(QA12+TMXDI)_p had a *DC* of 0.69. Their *DC*s also were higher than that in 40(UDMA)_p, which was 0.54. In addition, The *DC*s of 20(QA10+TMXDI)_p and 20(QA12+TMXDI)_p were higher than 0.55, which is recommended for clinical applications [57]. Thus, we can conclude that polymerization of 20(QA10+TMXDI)_m and 20(QA12+TMXDI)_m exhibited high efficiency and was not negatively influenced by a central benzene ring (which increases system stiffness [54]) and *N*-alkyl substituents (which increase the distance between polymerizing species [58,59]) present in their molecules.

A significant effect of the *N*-alkyl substituent on the density, volumetric contraction, glass temperature, water sorption, and leachability of 20(QA10+TMXDI)_p and 20(QA12+TMXDI)_p was not observed (Tables 8 and 9). 20(QA10+TMXDI)_p had a *d_p* of 1.21 g/cm³, *S* of 7.04%, *T_g* of 53.46 °C, *WS* of 10.43 µg/mm³, and *SL* of 2.18 µg/mm³. 20(QA12+TMXDI)_p had a 1% lower *d_p*, and this change was statistically insignificant. The *S* and *T_g* statistically significantly increased, and these changes were 10% and 13%, respectively. The *WS* decreased statistically insignificantly by 1%, whereas the *SL* increased by 13% and this change was statistically significant. Although the decrease in the *WS* was insignificant, the chemical character of the copolymer surface can explain this change. 20(QA12+TMXDI)_p was characterized by a *WCA* of 91.30° (Table 9), which corresponds to a hydrophobic surface [60,61]. 20(QA12+TMXDI)_p had a statistically insignificantly lower *WS* and *WCA*. However, its *WCA* was 91.30°, which corresponds to a hydrophobic surface [60,61]. An effect of the *N*-alkyl substituent on the *SL* can be attributed to a higher *MW* of QA12+TMXDI compared to that of QA10+TMXDI. It is possible that a smaller number of unreacted monomer molecules leached out from 20(QA12+TMXDI)_p because of a higher *DC* compared to 20(QA10+TMXDI)_p. A similar effect was also observed in other work on the copolymer of Qan+TMDI [39].

The reference copolymer, 40(UDMA)_p, had a 7.42% *S*, which was within the range limited by the *S* of 20(QA10+TMXDI)_p and 20(QA12+TMXDI)_p (Table 8). Compared to 40(UDMA)_p, 20(QA10+TMXDI)_m had a 5% lower *S* and 20(QA12+TMXDI)_m had a 4% higher *S*, and both changes were statistically significant. The small scale of these differences suggests that the experimental and reference formulations had similar volumetric contractions caused by polymerization. Therefore, the potential DCRM matrices modified with QA10+TMXDI and QA12+TMXDI would probably have a marginal gap similar to common dental dimethacrylate copolymers [62].

The thermal behavior of 20(QA10+TMXDI)_p and 20(QA12+TMXDI)_p also was appropriate for their application in the potential DCRM matrix. On one hand, the experimental copolymers had a *T_g* of 53.46 and 60.30 °C, respectively. These *T_g*s were lower than the *T_g* of 40(UDMA)_p (62.97 °C). The difference in *T_g*s between the reference copolymer and 20(QA10+TMXDI)_p was 15% and was statistically significant, whereas that for 20(QA12+TMXDI)_p was 4% and was statistically insignificant (Table 8). However, the *T_g*s in both cases were higher than 50 °C. This is a highly satisfactory result because it means

that the experimental copolymers occur in a glassy state up to a temperature of at least 50 °C. Therefore, we can assume that the experimental copolymers would maintain constant mechanical performance over the entire temperature range in the oral cavity [63].

Compared to 40(UDMA)_p, which had a *WS* of 5.31 µg/mm³ and *SL* of 0.17 µg/mm³, the experimental copolymers had *WS*s almost twice as high and *SL*s approximately fourteen times higher (Table 9). These were statistically significant differences, but the values of the *WS* and *SL* were noticeably lower than those defined by ISO 4049, i.e., 40 µg/mm³ and 7.5 µg/mm³, respectively [46]. A higher *WS* (10.43 µg/mm³), which was determined for 20(QA10+TMXDI)_p, was 26% of the maximum recommended by the ISO standard, and a higher *SL*, which was determined for 20(QA12+TMXDI)_p (2.46 µg/mm³), was 33% of the maximum recommended by the ISO 4049 standard. This is a highly satisfactory outcome, as the hydrophilic QA groups usually cause an increase in a polymer's *WS* [39]. The increased *WS* and *SL* of the experimental copolymers showed that the QA groups promote interactions with water molecules, even though the *N*-alkyl substituent decreased the hydrophilicity of the copolymer surface. This was confirmed by the result achieved for 40(UDMA)_p, which was characterized by the lowest *WCA* (74.07°, Table 9), and thus its surface was the most hydrophilic [60].

The mechanical properties of 20(QA10+TMXDI)_p and 20(QA12+TMXDI)_p decreased as the *N*-alkyl substituent length increased. The *E*, *FS*, and *HB* for 20(QA10+TMXDI)_p were 3244.9 Mpa, 100.6 Mpa, and 234.8 Mpa, respectively. They decreased by 7%, 10%, and 17% for 20(QA12+TMXDI)_p (Table 10). Only the result for the *HB* was statistically significant. This led to the conclusion that hardness was the most sensitive to the *N*-alkyl chain extension, as its decline was the most pronounced.

40(UDMA)_p exhibited the *E*, *FS*, and *HB* of 3597.7 Mpa, 125.4 Mpa, and 225.9 Mpa, respectively. Its modification by introducing QAUDMA resulted in statistically significant decreases of *E*, by 10 and 16%, and *FS*, by 20 and 28%, respectively, for 20(QA10+TMXDI)_p and 20(QA12+TMXDI)_p. The *HB* of 20(QA10+TMXDI)_p increased by 4% and this difference was statistically significant. As the length of the *N*-alkyl substituent increased to twelve carbon atoms, the *HB* decreased statistically significantly by 14%. However, the overall mechanical performance of 20(QA10+TMXDI)_p as well as 20(QA12+TMXDI)_p was fully satisfactory, as the tested parameters were high.

Finally, the experimental copolymers revealed antibacterial activity against *S. aureus* and *E. coli* (Table 11). 20(QA10+TMXDI)_p had a lower *MIC* and *MBC* than 20(QA12+TMXDI)_p. This means that the extension of the *N*-alkyl substituent in the QAUDMA with two methylene groups decreased the copolymer's antibacterial activity. If compared to 40(UDMA)_p, both copolymers had higher antibacterial activity. In addition, intra-species differences were observed for 20(QA12+TMXDI)_p. If compared to 40(UDMA)_p, 20(QA12+TMXDI)_p showed the same antibacterial activity concerning *S. aureus*, and greater antibacterial activity concerning *E. coli*. 20(QA12+TMXDI)_p had a *MBC* 50% lower and *MIC* 75% lower than 40(UDMA)_p in tests against *E. coli*. 20(QA10+TMXDI)_p showed more significant antibacterial activity and differentiation according to bacterial strain was no longer observed. 20(QA10+TMXDI)_p had a 75% lower *MBC* and 87.5% lower *MIC* than 40(UDMA)_p in tests against both bacteria strains.

We can additionally characterize the experimental copolymers using a common classification of antimicrobials as bactericidal or bacteriostatic. This classification assumes that if the *MBC* to *MIC* ratio is lower than four, a biocide can be recognized bactericidal, and if the *MBC* to *MIC* ratio is higher than six, a biocide can be recognized bacteriostatic [64]. As this ratio for 20(QA10+TMXDI)_p was two, one can assume this copolymer is bactericidal and it may be possible to administer the 20(QA10+TMXDI)_p dosages to kill 99.9% of the bacteria.

5. Conclusions

The two novel quaternary ammonium urethane-dimethacrylate (QAUDMA) monomers were successfully synthesized from 1,3-bis(1-isocyanato-1-methylethyl)benzene TMXDI and 2-(methacryloyloxy)ethyl-2-alkylhydroxyethylmethylammonium bromides with the decyl and

dodecyl *N*-alkyl substituents, respectively, QA10+TMXDI and QA12+TMXDI. The TMXDI diisocyanate provided an aromatic central ring in the QAUDMA structure.

The achieved QAUDMAs were used as comonomers 20 wt.% in the copolymerization with common dental dimethacrylates, UDMA 20 wt.%, Bis-GMA 40 wt.%, and TEGDMA 20 wt.%. For comparison, the UDMA 40 wt.%, Bis-GMA 40 wt.%, and TEGDMA 20 wt.% representative dental copolymer was also prepared.

The monomer compositions had adequate flowability and transparency required for dental materials.

A comparative analysis of the tested copolymers' properties showed that their polymerization shrinkage, glass transition temperature, and mechanical properties, were satisfactory and were usually similar to the properties of the reference copolymer. The water sorption and water solubility mostly deteriorated; however, they were satisfactory. Their values were far below the limits pointed at the international standard ISO 4049.

The antibacterial properties of the copolymers were characterized against *S. aureus* (ATCC 25923) and *E. coli* (ATCC 25922). The copolymer comprising QA10+TMXDI showed a significantly higher antibacterial effect than both the copolymer comprising QA12+TMXDI and the reference copolymer, as it had a lower minimum bactericidal concentration (MBC) and minimum inhibitory concentration (MIC).

This study demonstrated that the introduction of a benzene ring into the QAUDMA structure resulted in copolymers with very good physicochemical and mechanical characteristics and antibacterial activity. However, it was observed that the shorter the *N*-alkyl chain, the higher the antibacterial activity. Therefore, it is worth conducting further research with monomers that have shorter *N*-alkyl substituents. A more in-depth investigation of antibacterial properties should also be carried out for the tested copolymers, as the aim of this work was only to determine whether they have antibacterial activity.

Supplementary Materials: The following supporting information can be downloaded at: <https://www.mdpi.com/article/10.3390/ma17020298/s1>, Figure S1: DSC thermograms of copolymers: (a) 20(QA10+TMXDI)_p; (b) 20(QA12+TMXDI)_p; (c) 40(UDMA)_p, Figure S2: The goniometry camera images of deionized water droplets on the surfaces of copolymers: (a) 20(QA10+TMXDI)_p; (b) 20(QA12+TMXDI)_p; (c) 40(UDMA)_p, Figure S3: The results of antibacterial activity tests of 20(QA10+TMXDI)_p against *S. aureus* (ATCC 25923), Figure S4: The results of antibacterial activity tests of 20(QA12+TMXDI)_p against *S. aureus* (ATCC 25923), Figure S5: The results of antibacterial activity tests of 40(UDMA)_p against *S. aureus* (ATCC 25923), Figure S6: The results of antibacterial activity tests of 20(QA10+TMXDI)_p against *E. coli* (ATCC 25922), Figure S7: The results of antibacterial activity tests of 20(QA12+TMXDI)_p against *E. coli* (ATCC 25922), Figure S8: The results of antibacterial activity tests of 40(UDMA)_p against *E. coli* (ATCC 25922).

Author Contributions: Conceptualization, P.D. and I.B.-R.; Methodology, P.D. and I.B.-R.; Validation, P.D.; Formal analysis, I.B.-R.; Investigation, P.D. and M.C.-P.; Resources, P.D. and I.B.-R.; Data curation, P.D., A.K.-K. and G.C.; Writing—original draft, P.D. and I.B.-R.; Writing—review & editing, I.B.-R.; Visualization, P.D.; Supervision, A.K.-K., G.C. and I.B.-R.; Project administration, I.B.-R.; Funding acquisition, P.D. All authors have read and agreed to the published version of the manuscript.

Funding: This work was funded by the Polish Budget Funds for Scientific Research in 2023 as core funding for research and development activities at the Silesian University of Technology – funding for young scientists grant number 04/040/BKM23/0258.

Institutional Review Board Statement: Not applicable.

Informed Consent Statement: Not applicable.

Data Availability Statement: Data are contained within the article and supplementary materials.

Conflicts of Interest: The authors declare no conflicts of interest. The funders had no role in the design of the study, in the collection, analyses, or interpretation of data, in the writing of the manuscript, or in the decision to publish the results.

References

1. WHO. *Global Oral Health Status Report: Towards Universal Health Coverage for Oral Health by 2030*; World Health Organization: Geneva, Switzerland, 2022.
2. Wen, P.; Chen, M.; Zhong, Y.; Dong, Q.; Wong, H. Global Burden and Inequality of Dental Caries, 1990 to 2019. *J. Dent. Res.* **2022**, *101*, 392–399. [[CrossRef](#)]
3. Chen, L.; Suh, B.; Yang, J. Antibacterial dental restorative materials: A review. *Am. J. Dent.* **2018**, *31*, 6B–12B. [[PubMed](#)]
4. Beyth, N.; Farah, S.; Domb, A.; Weiss, E. Antibacterial dental resin composites. *Reac. Funct. Polym.* **2014**, *75*, 81–88. [[CrossRef](#)]
5. Ferrando-Magraner, E.; Bellot-Arcís, C.; Paredes-Gallardo, V.; Almerich-Silla, J.M.; García-Sanz, V.; Fernández-Alonso, M.; Montiel-Company, J.M. Antibacterial Properties of Nanoparticles in Dental Restorative Materials. A Systematic Review and Meta-Analysis. *Medicina* **2020**, *56*, 55. [[CrossRef](#)] [[PubMed](#)]
6. Domb, A.J.; Weiss, E.; Beyth, N.; Farber, I.; Perez-Davidi, M. Antimicrobial Nanoparticulate Additives Forming Non-Leachable Sustained Antimicrobial Polymeric Compositions. U.S. Patent 20080226728A1, 18 September 2008.
7. Fernandes, J.; Menezes, V.; Albuquerque, A.; Oliveira, M.; Meira, K.; Menezes, R., Jr.; Sampaio, F.C. Improving Antimicrobial Activity of Dental Restorative Materials. In *Emerging Trends in Oral Health Sciences and Dentistry*; InTech: London, UK, 2015.
8. Badr, S.; Abdulrahman, A.; Abdullah, A.; Essam, A.; Mohammad, Y.; Shahzeb, H. Effect of various antibacterial materials in dental composites: A systematic review. *Ann. Dent. Spec.* **2021**, *9*, 39–44.
9. Mehdawi, I.; Young, A. Antibacterial composite restorative materials for dental applications. In *Non-Metallic Biomaterials for Tooth Repair and Replacement*; Elsevier: Amsterdam, The Netherlands, 2013; pp. 270–293.
10. Zhou, X.; Huang, X.; Li, M.; Peng, X.; Wang, S.; Zhou, X.; Cheng, L. Development and status of resin composite as dental restorative materials. *J. Appl. Polym. Sci.* **2019**, *136*, 48180. [[CrossRef](#)]
11. Chan, D.; Hu, W.; Chung, K.; Larsen, R.; Jensen, S.; Cao, D.; Gaviria, L.; Ong, J.; Whang, K.; Eiampongpaiboon, T. Reactions: Antibacterial and bioactive dental restorative materials: Do they really work? *Am. J. Dent.* **2018**, *15*, 32B–36B.
12. Farrugia, C.; Camilleri, J. Antimicrobial properties of conventional restorative filling materials and advances in antimicrobial properties of composite resins and glass ionomer cements—A literature review. *Dent. Mater.* **2015**, *31*, e89–e99. [[CrossRef](#)]
13. Ibrahim, M.; Garcia, I.; Kensara, A.; Balhaddad, A.; Collares, F.; Williams, M.; Ibrahim, A.; Lin, N.; Weir, M.; Xu, H.; et al. How we are assessing the developing antibacterial resin-based dental materials? A scoping review. *J. Dent.* **2020**, *99*, 103369. [[CrossRef](#)]
14. Chen, Z.; Chu, Z.; Jiang, Y.; Xu, L.; Qian, H.; Wang, Y.; Wang, W. Recent advances on nanomaterials for antibacterial treatment of oral diseases. *Mater. Today Bio.* **2023**, *20*, 100635. [[CrossRef](#)]
15. Zhang, Y.; Chen, Y.; Hu, Y.; Huang, F.; Xiao, Y. Quaternary ammonium compounds in dental restorative materials. *Dent. Mater. J.* **2018**, *37*, 183–191. [[CrossRef](#)] [[PubMed](#)]
16. Sun, Q.; Zhang, L.; Bai, R.; Zhuang, Z.; Zhang, Y.; Yu, T.; Peng, L.; Xin, T.; Chen, S.; Han, B. Recent Progress in Antimicrobial Strategies for Resin-Based Restoratives. *Polymers* **2021**, *13*, 1590. [[CrossRef](#)] [[PubMed](#)]
17. Ramburrun, P.; Pringle, N.; Dube, A.; Adam, R.; D'Souza, S.; Aucamp, M. Recent Advances in the Development of Antimicrobial and Antifouling Biocompatible Materials for Dental Applications. *Materials* **2021**, *14*, 3167. [[CrossRef](#)]
18. Makvandi, P.; Jamaledin, R.; Jabbari, M.; Nikfarjam, N.; Borzacchiello, A. Antibacterial Quaternary Ammonium Compounds in Dental Materials: A Systematic Review. *Dent. Mater.* **2018**, *34*, 851–867. [[CrossRef](#)] [[PubMed](#)]
19. Ge, Y.; Wang, S.; Zhou, X.; Wang, H.; Xu, H.H.K.; Cheng, L. The Use of Quaternary Ammonium to Combat Dental Caries. *Materials* **2015**, *8*, 3532–3549. [[CrossRef](#)] [[PubMed](#)]
20. Imazato, S.; Chen, J.H.; Ma, S.; Izutani, N.; Li, F. Antibacterial Resin Monomers Based on Quaternary Ammonium and Their Benefits in Restorative Dentistry. *Jap. Dent. Sci. Rev.* **2012**, *48*, 115–125. [[CrossRef](#)]
21. Featherstone, J. Dental restorative materials containing quaternary ammonium compounds have sustained antibacterial action. *J. Am. Dent. Assoc.* **2022**, *153*, 1114–1120. [[CrossRef](#)]
22. Li, Y.; Li, B.; Guo, X.; Wang, H.; Cheng, L. Applications of quaternary ammonium compounds in the prevention and treatment of oral diseases: State-of-the-art and future directions. *J. Dent.* **2023**, *137*, 104678. [[CrossRef](#)]
23. Jiao, Y.; Niua, L.; Maa, S.; Li, J.; Tayd, F.; Chena, J. Quaternary ammonium-based biomedical materials: State-of-the-art, toxicological aspects and antimicrobial resistance. *Prog. Polym. Sci.* **2017**, *71*, 53–90. [[CrossRef](#)]
24. Mousavinasab, S. Biocompatibility of composite resins. *Dent. Res. J.* **2011**, *8*, S21–S29.
25. Santos, M.R.E.; Fonseca, A.C.; Mendonça, P.V.; Branco, R.; Serra, A.C.; Morais, P.V.; Coelho, J.F.J. Recent Developments in Antimicrobial Polymers: A Review. *Materials* **2016**, *9*, 599. [[CrossRef](#)] [[PubMed](#)]
26. Capita, R.; Alonso-Calleja, C. Antibiotic-resistant bacteria: A challenge for the food industry. *Crit. Rev. Food Sci. Nutr.* **2013**, *53*, 11–48. [[CrossRef](#)] [[PubMed](#)]
27. Chinemerem, D.; Ugwu, M.; Oliseloke, A.; Al-Ouqaili, M.; Chinedu, I.; Victor, C.; Saki, M. Antibiotic resistance: The challenges and some emerging strategies for tackling a global menace. *J. Clin. Lab. Anal.* **2022**, *36*, e24655. [[CrossRef](#)]
28. Saha, M.; Sarkar, A. Review on Multiple Facets of Drug Resistance: A Rising Challenge in the 21st Century. *J. Xenobiot.* **2021**, *11*, 197–214. [[CrossRef](#)] [[PubMed](#)]
29. Huang, L.; Xiao, Y.H.; Xing, X.D.; Li, F.; Ma, S.; Qi, L.L.; Chen, J.H. Antibacterial Activity and Cytotoxicity of Two Novel Cross-Linking Antibacterial Monomers on Oral Pathogens. *Arch. Oral Biol.* **2011**, *56*, 367–373. [[CrossRef](#)] [[PubMed](#)]

30. Huang, L.; Yu, F.; Sun, X.; Dong, Y.; Lin, P.T.; Yu, H.H.; Xiao, Y.H.; Chai, Z.G.; Xing, X.D.; Chen, J.H. Antibacterial Activity of a Modified Unfilled Resin Containing a Novel Polymerizable Quaternary Ammonium Salt MAE-HB. *Sci. Rep.* **2016**, *6*, 33858. [[CrossRef](#)]
31. Manouchehri, F.; Sadeghi, B.; Najafi, F.; Mosslemin, M.H.; Niakan, M. Synthesis and Characterization of Novel Polymerizable Bis-Quaternary Ammonium Dimethacrylate Monomers with Antibacterial Activity as an Efficient Adhesive System for Dental Restoration. *Polym. Bull.* **2019**, *76*, 1295–1315. [[CrossRef](#)]
32. Makvandi, P.; Ghaemy, M.; Mohseni, M. Synthesis and Characterization of Photo-Curable Bis-Quaternary Ammonium Dimethacrylate with Antimicrobial Activity for Dental Restoration Materials. *Eur. Polym. J.* **2016**, *74*, 81–90. [[CrossRef](#)]
33. Liang, X.; Söderling, E.; Liu, F.; He, J.; Lassila, L.V.J.; Vallittu, P.K. Optimizing the Concentration of Quaternary Ammonium Dimethacrylate Monomer in Bis-GMA/TEGDMA Dental Resin System for Antibacterial Activity and Mechanical Properties. *J. Mater. Sci. Mater. Med.* **2014**, *25*, 1387–1393. [[CrossRef](#)]
34. Huang, Q.T.; He, J.W.; Lin, Z.M.; Liu, F.; Lassila, L.V.J.; Vallittu, P.K. Physical and Chemical Properties of an Antimicrobial Bis-GMA Free Dental Resin with Quaternary Ammonium Dimethacrylate Monomer. *J. Mech. Behav. Biomed. Mater.* **2016**, *56*, 68–76. [[CrossRef](#)]
35. Liang, X.; Huang, Q.; Liu, F.; He, J.; Lin, Z. Synthesis of Novel Antibacterial Monomers (UDMQA) and Their Potential Application in Dental Resin. *J. Appl. Polym. Sci.* **2013**, *129*, 3373–3381. [[CrossRef](#)]
36. Huang, Q.; Lin, Z.; Liang, X.; Liu, F.; He, J. Preparation and Characterization of Antibacterial Dental Resin with UDMQA-12. *Adv. Polym. Technol.* **2014**, *33*, 21395. [[CrossRef](#)]
37. Chrószcz, M.W.; Barszczewska-Rybarek, I.M. Synthesis and Characterization of Novel Quaternary Ammonium Urethane-Dimethacrylate Monomers—A Pilot Study. *Int. J. Mol. Sci.* **2021**, *22*, 8842. [[CrossRef](#)]
38. Chrószcz, M.W.; Barszczewska-Rybarek, I.M.; Kazek-Kęsik, A. Novel Antibacterial Copolymers Based on Quaternary Ammonium Urethane-Dimethacrylate Analogues and Triethylene Glycol Dimethacrylate. *Int. J. Mol. Sci.* **2022**, *23*, 4954. [[CrossRef](#)]
39. Chrószcz-Porebska, M.W.; Barszczewska-Rybarek, I.M.; Chladek, G. Characterization of the Mechanical Properties, Water Sorption, and Solubility of Antibacterial Copolymers of Quaternary Ammonium Urethane-Dimethacrylates and Triethylene Glycol Dimethacrylate. *Materials* **2022**, *15*, 5530. [[CrossRef](#)]
40. Chrószcz-Porebska, M.; Kazek-Kęsik, A.; Chladek, G.; Barszczewska-Rybarek, I. Novel mechanically strong and antibacterial dimethacrylate copolymers based on quaternary ammonium urethane-dimethacrylate analogues. *Dent. Mater.* **2023**, *39*, 659–664. [[CrossRef](#)]
41. Chrószcz-Porebska, M.W.; Barszczewska-Rybarek, I.M.; Kazek-Kęsik, A.; Ślęzak-Prochazka, I. Cytotoxicity and Microbiological Properties of Copolymers Comprising Quaternary Ammonium Urethane-Dimethacrylates with Bisphenol A Glycerolate Dimethacrylate and Triethylene Glycol Dimethacrylate. *Materials* **2023**, *16*, 3855. [[CrossRef](#)]
42. Chrószcz-Porebska, M.W.; Barszczewska-Rybarek, I.M.; Chladek, G. Physicochemical Properties of Novel Copolymers of Quaternary Ammonium UDMA Analogues, Bis-GMA, and TEGDMA. *Int. J. Mol. Sci.* **2023**, *24*, 1400. [[CrossRef](#)]
43. ISO 4049:2019; Plastics—Resins in the Liquid State or As Emulsions or Dispersions—Determination of Apparent Viscosity Using A Single Cylinder Type Rotational Viscometer Method. International Organization for Standardization: Geneva, Switzerland, 2019.
44. ISO 489:2022; Plastics—Determination of Refractive Index. International Organization for Standardization: Geneva, Switzerland, 2022.
45. ISO 11357-2:2020; Plastics—Differential Scanning Calorimetry (DSC)—Part 2: Determination of Glass Transition Temperature and Step Height. International Organization for Standardization: Geneva, Switzerland, 2020.
46. ISO 4049:2019; Dentistry—Polymer-Based Restorative Materials. International Organization for Standardization: Geneva, Switzerland, 2019.
47. ISO 2039-1:2001; Plastics—Determination of Hardness—Part 1: Ball Indentation Method. International Organization for Standardization: Geneva, Switzerland, 2001.
48. ISO 178:2019; Plastics—Determination of Flexural Properties. International Organization for Standardization: Geneva, Switzerland, 2019.
49. Barszczewska-Rybarek, I. Quantitative determination of degree of conversion in photocured poly(urethane-dimethacrylate)s by FTIR spectroscopy. *J. Appl. Polym. Sci.* **2012**, *123*, 1604–1611. [[CrossRef](#)]
50. Six, C.; Richter, F. Isocyanates, Organic. In *Ullmann's Encyclopedia of Industrial Chemistry*; Wiley-VCH: Weinheim, Germany, 2003; Volume 20, pp. 63–82.
51. Manappallil, J.J. *Basic Dental Materials*, 4th ed.; Jaypee Brothers Medical Publishers: New Delhi, India, 2015.
52. Oivanen, M.; Keulemans, F.; Garoushi, S.; Vallittu, P.; Lassila, L. The effect of refractive index of fillers and polymer matrix on translucency and color matching of dental resin composite. *Biomater. Investig. Dent.* **2021**, *8*, 48–53. [[CrossRef](#)]
53. Gonçalves, F.; Kawano, Y.; Pfeifer, C.; Stansbury, J.W.; Braga, R.R. Influence of BisGMA, TEGDMA, and BisEMA contents on viscosity, conversion, and flexural strength of experimental resins and composites. *Eur. J. Oral Sci.* **2009**, *117*, 442–446. [[CrossRef](#)]
54. Stansbury, J.W. Dimethacrylate network formation and polymer property evolution as determined by the selection of monomers and curing conditions. *Dent. Mater.* **2012**, *28*, 13–22. [[CrossRef](#)]
55. Du, M.; Zheng, Y. Degree of conversion and mechanical properties studies of UDMA based materials for producing dental posts. *Polym. Compos.* **2008**, *29*, 623–630. [[CrossRef](#)]

56. Moldovan, M.; Balazsi, R.; Soanca, A.; Roman, A.; Sarosi, C.; Prodan, D.; Vlassa, M.; Cojocaru, I.; Saceleanu, V.; Cristescu, I. Evaluation of the Degree of Conversion, Residual Monomers and Mechanical Properties of Some Light-Cured Dental Resin Composites. *Materials* **2019**, *12*, 2109. [[CrossRef](#)]
57. Alshali, R.Z.; Silikas, N.; Satterthwaite, J.D. Degree of conversion of bulk-fill compared to conventional resin-composites at two time intervals. *Dent. Mater.* **2013**, *29*, e213–e217. [[CrossRef](#)]
58. Nuzhdina, A.V.; Morozov, A.S.; Kopitsyna, M.N.; Strukova, E.N.; Shlykova, D.S.; Bessonov, I.V.; Lobakova, E.S. Simple and Versatile Method for Creation of Non-Leaching Antimicrobial Surfaces Based on Cross-Linked Alkylated Polyethyleneimine Derivatives. *Mater. Sci. Eng. C* **2017**, *70*, 788–795. [[CrossRef](#)]
59. Yudovin-Farber, I.; Beyth, N.; Weiss, E.I.; Domb, A.J. Antibacterial Effect of Composite Resins Containing Quaternary Ammonium Polyethyleneimine Nanoparticles. *J. Nanopart Res.* **2010**, *12*, 591–603. [[CrossRef](#)]
60. Law, K.-Y. Definitions for Hydrophilicity, Hydrophobicity, and Superhydrophobicity: Getting the Basics Right. *J. Phys. Chem. Lett.* **2014**, *5*, 686–688. [[CrossRef](#)]
61. Grainger, D.; Castner, D. 3.301—Surface Analysis and Biointerfaces: Vacuum and Ambient in Situ Techniques. In *Comprehensive Biomaterials*; Ducheyne, P., Ed.; Elsevier: Amsterdam, The Netherlands, 2011; pp. 1–22.
62. Susila, A.V. Role of Composition on Polymerization Shrinkage and Shrinkage Stress in Dental Composites. *J. Oper. Dent. Endod.* **2021**, *6*, 31–44.
63. Moraes, J.C.S.; Sostena, M.M.D.S.; Roberto, C. The Glass Transition Temperature in Dental Composites. In *Metal, Ceramic and Polymeric Composites for Various Uses*; Chapter 33; John Cuppoletti, J., Ed.; IntechOpen: London, UK, 2011.
64. Davis, J.L. Pharmacologic Principles. In *Equine Internal Medicine*, 4th ed.; Reed, S.M., Bayly, W.M., Sellon, D.C., Eds.; Elsevier Inc.: Philadelphia, PA, USA, 2018; pp. 79–137.

Disclaimer/Publisher’s Note: The statements, opinions and data contained in all publications are solely those of the individual author(s) and contributor(s) and not of MDPI and/or the editor(s). MDPI and/or the editor(s) disclaim responsibility for any injury to people or property resulting from any ideas, methods, instructions or products referred to in the content.